Phytomedicine Plus 5 (2025) 100908

Contents lists available at ScienceDirect

Phytomedicine Plus

journal homepage: www.sciencedirect.com/journal/phytomedicine-plus

Metabolite profiling, cytotoxicity, liver ROS detoxifiers and acetylcholinesterase inhibitors from *Trachyandra ciliata* L.F. (Kunth) (wild cabbage)

Sihle Ngxabi [a,*], Avela Sogoni [a], Nasifu Kerebba [b,c], Rialet Pieters [d], Suranie Horn [e], John P. Giesy [f,g,h], Learnmore Kambizi [a], Charles Petrus Laubscher [a], Muhali Olaide Jimoh [a]

[a] Department of Horticultural Sciences, Faculty of Applied Sciences, Cape Peninsula University of Technology, Bellville 7535, South Africa
[b] Department of Chemistry, Makerere University, Kampala 7062, Uganda
[c] Department of Physical Sciences, School of Natural and Applied Sciences, P.O. Box 2000, Kansanga Kampala, Uganda
[d] Unit for Environmental Sciences and Management, Faculty of Natural and Agricultural Sciences, North-West University, Private Bag X6001, Potchefstroom, North West 2520, South Africa
[e] Occupational Hygiene and Health Research Initiative, Faculty of Health Science, North-West University, Private Bag X6001, Potchefstroom, North West 2520, South Africa
[f] Department of Biomedical Veterinary Sciences and Toxicology Centre, University of Saskatchewan, Saskatoon, SK S7N 5B3, Canada
[g] Department of Integrative Biology and Center for Integrative Toxicology, Michigan State University, East Lansing, MI 48824, USA
[h] Department of Environmental Science, Baylor University, Waco, TX, USA

ARTICLE INFO

Keywords:
Acetylcholine
Alzheimer's disease
Bioactive compounds
Cancer
Dementia
Halophytes
Liver disorders
Salinity

ABSTRACT

Introduction: Wild cabbage (*Trachyandra ciliata*) is one of the understudied, wild, edible halophytes from South Africa. Although its edibility has recently been validated, its therapeutic potential was yet to be explored. This research was carried out to profile and characterise the phytochemical content of *T. ciliata* extracts and evaluate its potential as a therapeutic agent for cancer, acetylcholinesterase (AChE) inhibition and reactive oxygen species (ROS) scavenging in the liver.

Methods: Cuttings of *T. ciliata* were grown under 0, 50, 100, 150, and 200 mM salinity concentrations. The ultra-high-performance liquid chromatography mass spectrometry (UHPLC-MS) was employed to quantify and characterise metabolites in leaves, roots, and flower buds of *T. ciliata*. The yellow dye 3-(4,5-dimethyltiazol-2yl)-2,5-diphenyl tetrazolium bromide (MTT), Ellman's colourimetric method, and the 2′,7′-dichlorodihydrofluorescein diacetate assay (H_2DCF-DA) were respectively employed to evaluate cytotoxicity, AChE antagonism, and ROS scavenging of the extracts of *T. ciliata*.

Results: A total of 71 compounds were observed, which were grouped into flavonoids, anthocyanins, alkaloids, nucleobase, nucleosides/tide, saccharides, fatty acids, amino acids, and coumarins. A concentration of 1 mg/mL of extracts of *T. ciliata* flower buds prepared from plants grown at 0 mM and 100 mM salinity, showed strong cytotoxicity to cancer cells, however, the extracts also had moderate and weak cytotoxicity to non-cancer cells. All extracts inhibited AChE activity. Moreover, ROS scavenging was mainly observed primarily in the extracts of leaves from plants grown at all salinities, and in the extract of roots from plants grown at 0 mM salinity treatment.

Conclusion: A maiden documentation of anticancer, acetylcholinesterase inhibition, and ROS scavenging activity of crude extracts of *T. ciliata* was achieved in this study. These findings suggest that *T. ciliata* could be a potential therapeutic agent for the treatment of cancer, Alzheimer's disease, and liver disorders, amidst the quest to develop more plant-based pharmaceuticals for the treatment of chronic diseases.

* Corresponding author.
E-mail address: Ngxabis@cput.ac.za (S. Ngxabi).

https://doi.org/10.1016/j.phyplu.2025.100908

Available online 26 October 2025

1. Introduction

Chronic diseases are distinguished by their non-infectious nature, numerous risk factors, extended development period, extended temporal course of development, functional damage or disability, and incurability (Piovani et al., 2022; Abdullahi et al., 2025). Annually, chronic diseases are accountable for over 41 million deaths, which constitute 74 % of all fatalities worldwide, while millions more people live with non-communicable diseases (NCDs), and have a reduced quality of life (Piovani et al., 2022). Chronic diseases that cause significant death and disability include neurological and mental health disorders, cancer, cardiovascular diseases, diabetes, substance abuse-induced liver disorders, and gastrointestinal disorders, among others (Babashahi et al., 2021; Chen et al., 2025).

The distress and severity of cancer especially at advanced stage makes it a significant global health issue, accounting for the second highest cause of deaths in the current millennium, with more than 10 million deaths reported in 2020 (Lucero-Prisno et al., 2023; Mohammed et al., 2023). As a result, one of the Sustainable Development Goals for lowering early mortality from non-communicable diseases is to reduce cancer mortality (Lucero-Prisno et al., 2023). Conventional cancer treatment includes surgery, chemotherapy, immunotherapy, and radiotherapy, all of which have limitations and accompanying complications, such as myelosuppression, gastrointestinal discomfort, liver and kidney toxicity, and heart damage (Venkatachalapathy et al., 2021; Zafar et al., 2025). The use of plant-based approaches is gaining popularity because they offer a potential complementary or alternative option, with some showing promise in lowering cancer risk or adverse effects (Ferreira et al., 2022; Lee et al., 2024).

Alzheimer's disease (AD), the most prevalent neurodegenerative disorder and the cause of adult-onset cognitive impairment generally termed dementia, is distinguished by a gradual loss of cognitive abilities accompanied by behavioural symptoms such as psychosis, agitation, depression, repetitive actions and uneven sleep patterns (Safiri et al., 2024). A proper equilibrium of neurotransmitter systems, including acetylcholine (ACh), is necessary for efficient cognitive function and AD prevention (Chen et al., 2022; Yang et al., 2023). In persons suffering from AD, acetylcholinesterase enzyme (AChE) is constantly located in proximity to amyloid deposits, which might have a role in the synthesis of amyloid proteins, which are characteristic of AD (Gajendra et al., 2024; Huang et al., 2022). Thus, (AChEIs) have been used as the principal treatment for dementia since the 1990s (Asghar et al., 2025; Gajendra et al., 2024; Sogoni et al., 2025a). However, synthetic pharmaceuticals that are commonly used to treat Alzheimer, such as donepezil, rivastigmine, and galantamine, can cause adverse effects, such as reduced heart rate, gastrointestinal difficulties and subsequent decreased appetite (De Oliveira et al., 2024; ALNasser et al., 2025). Hence, natural compounds derived from edible plants, including halophytes, have begun to gain recognition globally as promising AChE inhibitors, which could be employed as a therapeutic alternative for Alzheimer treatment (ALNasser et al., 2025; Islam et al., 2024; Taqui et al., 2022).

The liver is the primary biological producer of immune modulators, plasma proteins, blood coagulation factors, and protease inhibitors, while it also helps in the digestion and assimilation of nutrients from food, medications, alcohols, and xenobiotics (Dicks, 2024; Schulze et al., 2019). Liver disorders are often associated with excessive production of reactive oxygen species (ROS), which can cause oxidative stress to liver cells, proteins, and DNA (Lee et al., 2022). Therefore, it is crucial for cellular defence systems to maintain redox homeostasis (Huete-Acevedo et al., 2024; Sies, 2015). In recent years, the medicinal potential of plant extracts with high antioxidant qualities has drawn more attention due to the adverse effects presented by synthetic pharmaceuticals (Liu et al., 2023). For instance, phytochemicals such as apigenin (flavanone), peonidin (anthocyanin), adenosine (nucleoside), thioctic acid (carboxylic acid), scopoletin (coumarin), among other plant-based compounds, have been reported to possess high ROS scavenging activities that may be useful in the treatment or prevention of cardiovascular diseases (Liu et al., 2023).

Natural products derived from herbal remedies, medicinal plants, and functional foods, along with their constituents, have been utilised for the treatment of various diseases, such as cancer, neurodegenerative diseases, liver disorders, diabetes, and gastrointestinal diseases from ancient times to the present day (Asong et al., 2019; Cock et al., 2021; Gonfa et al., 2023; Kim et al., 2018). Notably, halophytes have been utilised for medicinal purposes across different countries and have demonstrated effectiveness in preventing and managing chronic diseases that afflict modern societies (Mohammed et al., 2023). There is a growing focus on these species due to their rich content of bioactive compounds, including primary and secondary metabolites like phenolic acids and their derivatives, polyunsaturated fatty acids, vitamins, flavonoids, anthocyanins, alkaloids, nucleobases, saccharides, amino acids, and coumarins, amongst others (Ferreira et al., 2022; Lee et al., 2024). Despite the increasing global interest in exploring the medicinal properties of halophytes in recent years, South African halophytes have largely been underutilized as potential agents in the amelioration of chronic diseases (Cock, 2015; Sogoni et al., 2025b).

The edible plant, wild cabbage (*Trachyandra ciliata*) is one of the lesser-studied halophytes from South Africa (Ngxabi et al., 2024). A recent study by Ngxabi et al. (2025) validated its edibility and reported that salinity improved its nutritional composition and antioxidant capacity. However, its chemical constituents and pharmacological potential remained undocumented. The flower buds of *T. ciliata* are edible and were historically consumed as a vegetable by the *Khoi-San* people who inhabited the coastal areas of the Western Cape region of South Africa (De Vynck et al., 2016; Ngxabi et al., 2024). Although the edibility of flower buds was reported recently (Ngxabi et al., 2025), it is crucial to explore other plant parts for potential therapeutic properties to maximize their use and promote their medicinal importance. There are currently no studies in the literature that have characterized diverse compounds of this plant and explored the biological activity of its crude extracts. Thus, for the first time, this research was carried out to profile and characterize the phytochemical content of *T. ciliata* extracts and evaluate its pharmacological potential for cancer management, acetylcholinesterase inhibition and ROS scavenging in the liver.

2. Materials and methods

2.1. Greenhouse experimental design

The experiment was conducted at the greenhouse nursery at the Bellville campus of the Cape Peninsula University of Technology, in Cape Town, South Africa. The greenhouse conditions and propagation procedures were identical to those described in Ngxabi et al. (2025). *Trachyandra ciliata* was identified by Prof. Charles Laubscher and allocated a voucher number 6163 at the Cape Peninsula University of Technology Herbarium, Bellville. The plant material was obtained from the nursery of the Cape Peninsula University of Technology, Bellville campus. Plants were subsequently grown under five salinities with concentrations of 0, 50, 100, 150, or 200 mM NaCl. Following 15 weeks of growth under saline conditions, leaves, roots, and flower buds were harvested, dried, and ground for extraction and further analyses. Higher salinity concentrations (150 and 200 mM NaCl) did not produce any flower buds, due to oxidative stress caused by NaCl (Ngxabi et al., 2025).

2.2. Extraction protocol

The extraction was carried out using a method outlined by Jimoh et al. (2024). Briefly, 10 g of pulverized plant material was weighed and added to 200 mL 70 % ethanol in a round bottom flask. After two days of vigorous shaking at 120 rpm (rpm) on an orbital shaker (Orbital Incubator Shaker, Gallenkamp), the mixture was vacuum-filtered through

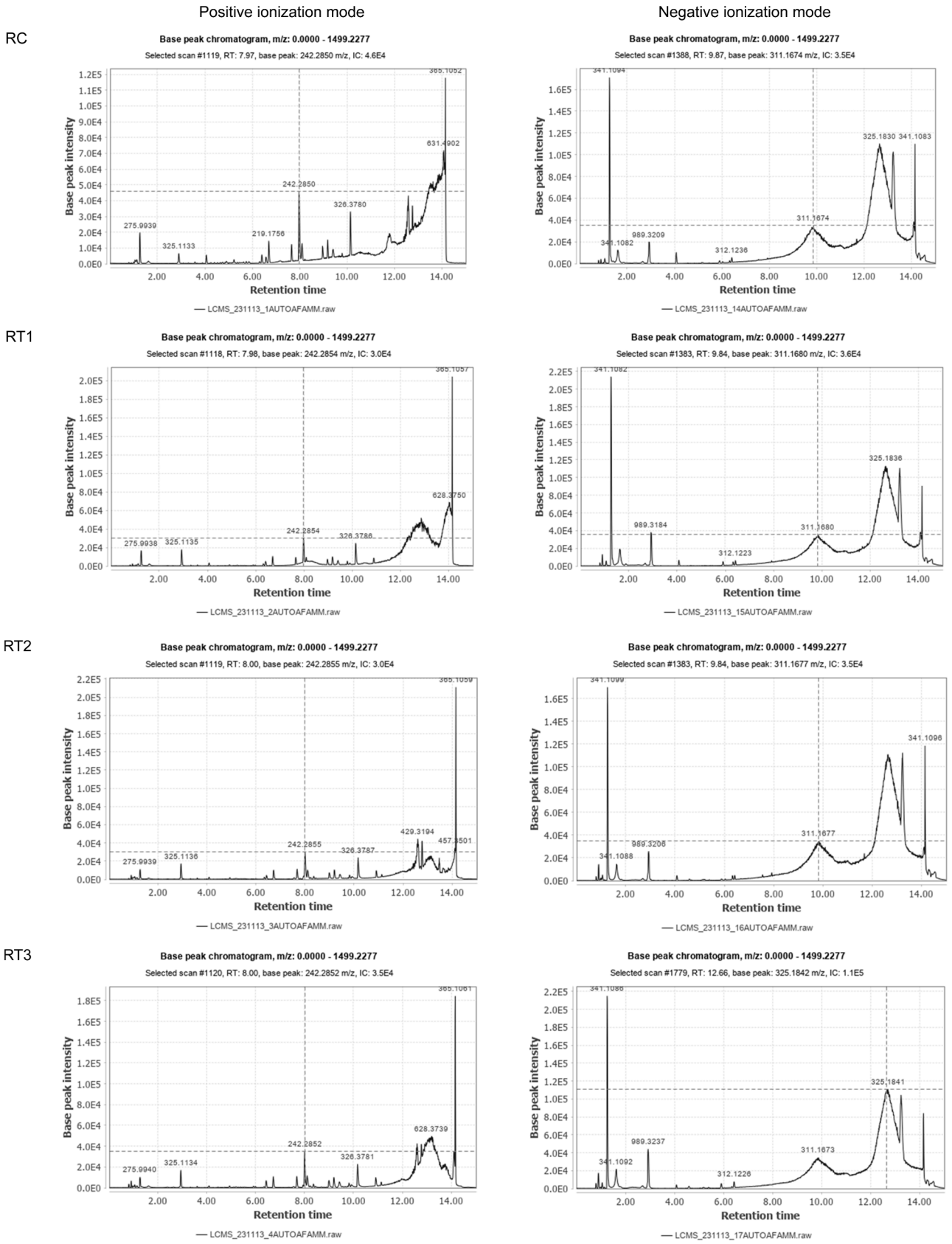

Fig. 1. UHPLC-ESI-MS base peak chromatogram of T. ciliata leaves, roots, and flower bud extracts analysed in the ESI negative and positive modes.

RT4

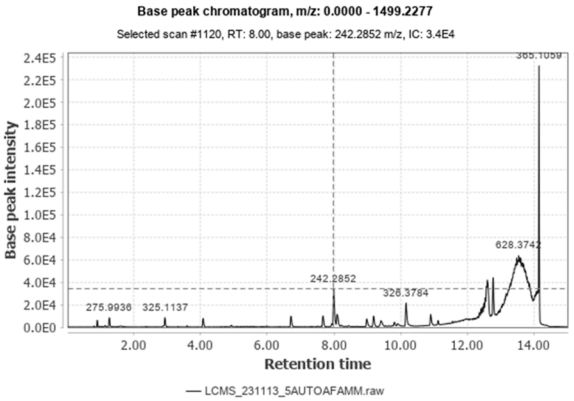

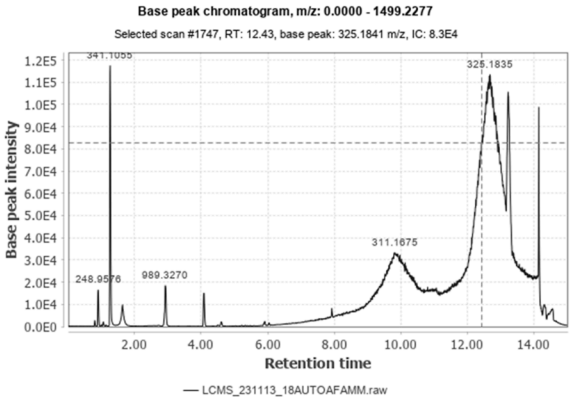

FC

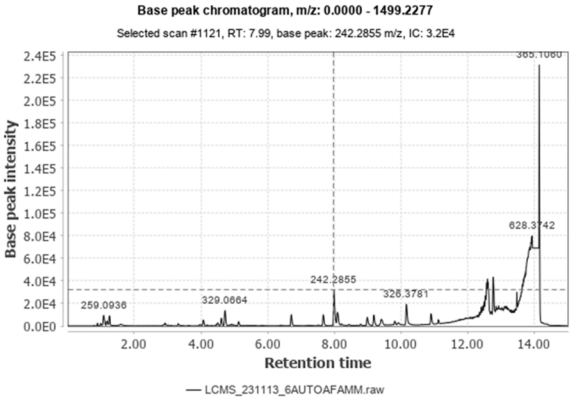

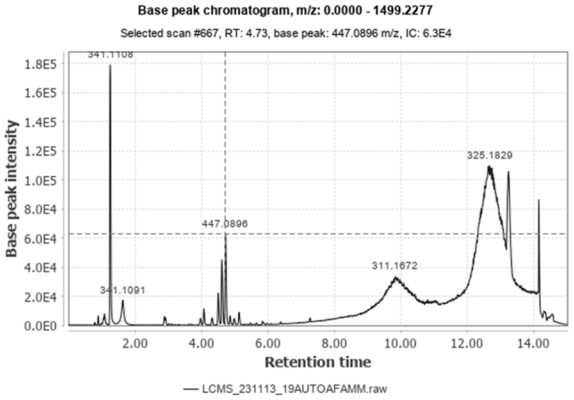

FT1

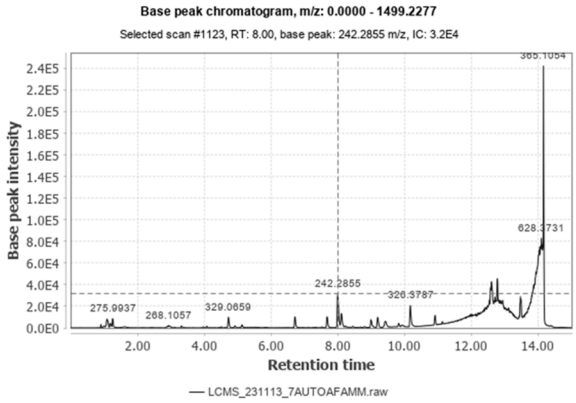

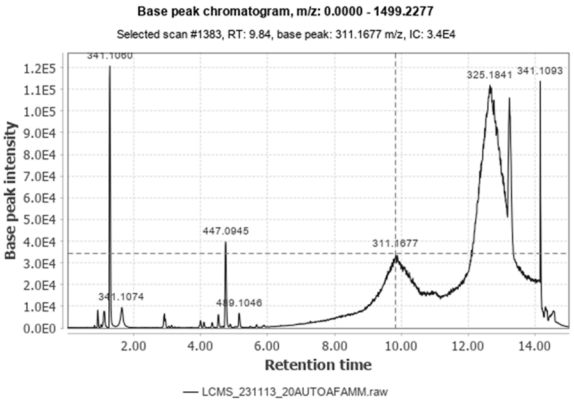

FT2

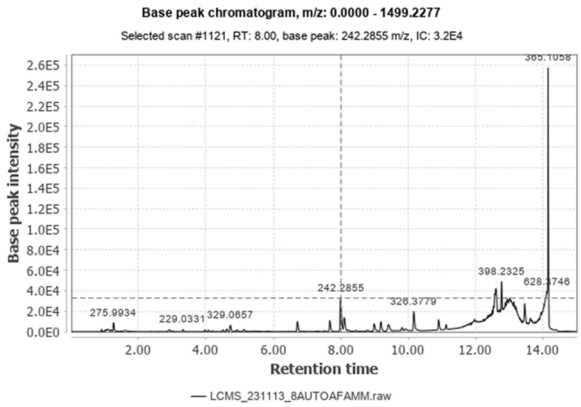

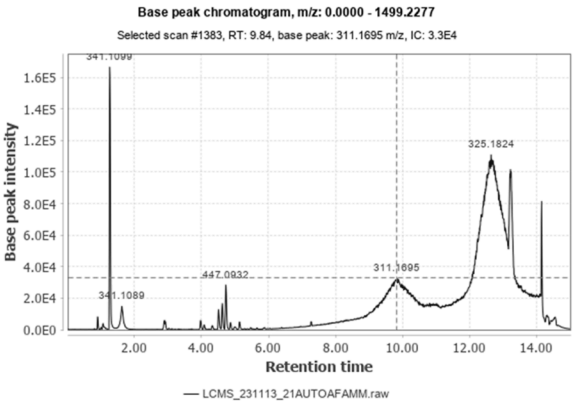

Fig. 1. (*continued*).

LC

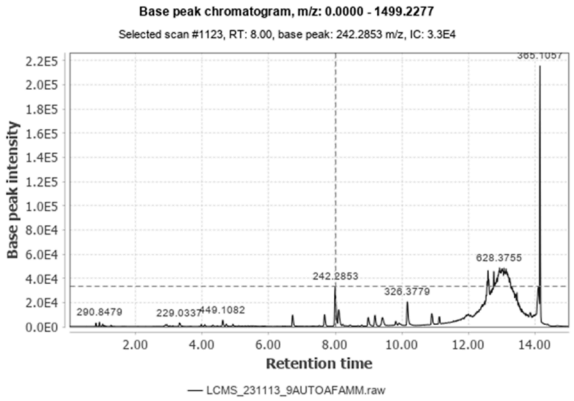

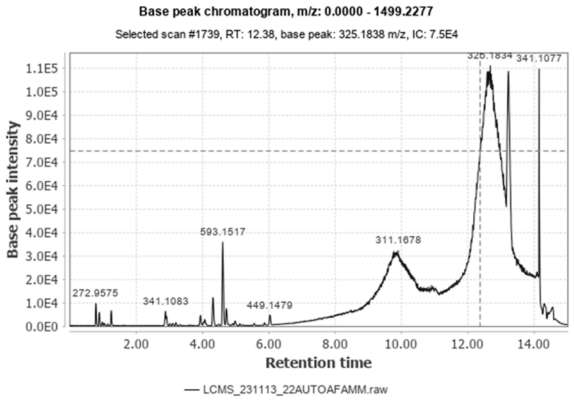

LT1

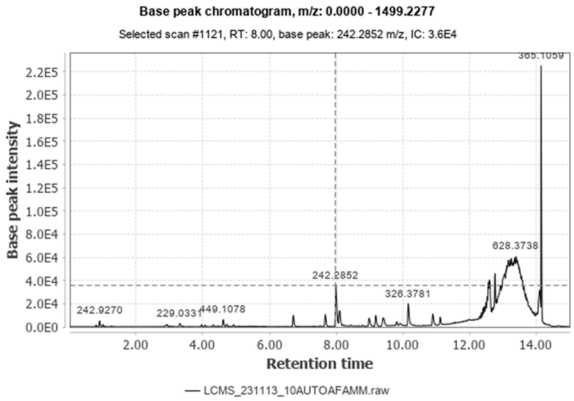

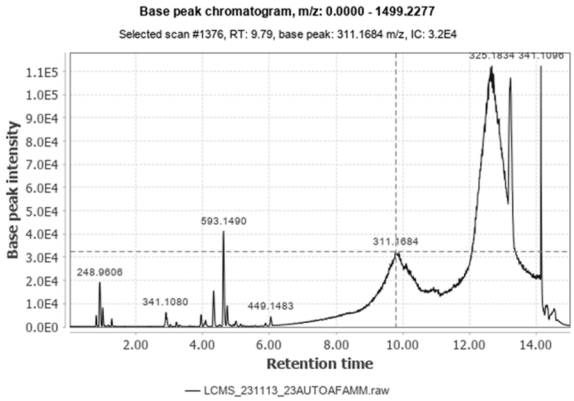

LT2

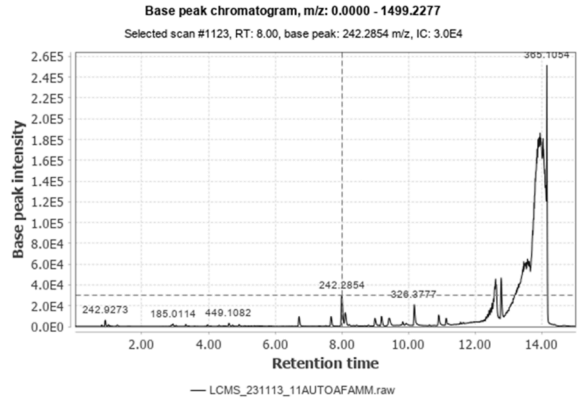

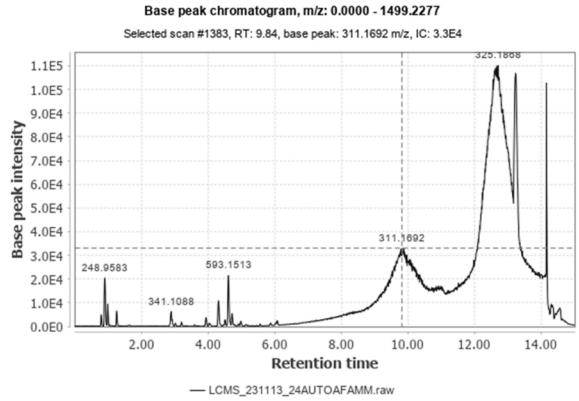

LT3

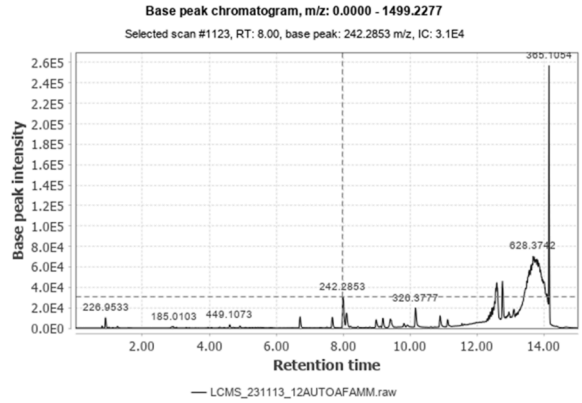

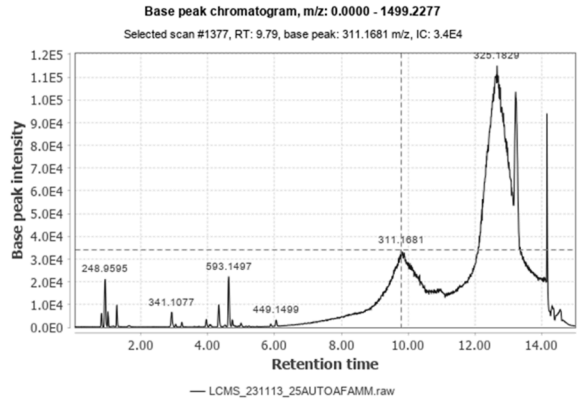

Fig. 1. (*continued*).

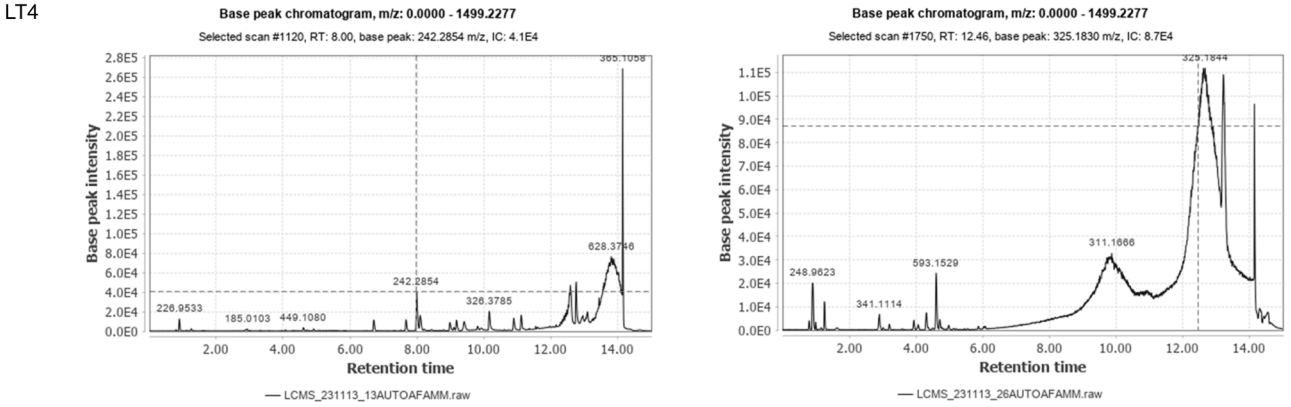

Fig. 1. (*continued*).

Whatman No. 1 filter paper in a Buchner funnel. The crude extract was concentrated and dried by eliminating excess ethanol from the filtrate using a rotary evaporator (Strike-202 Steroglass, Italy) set to 78 °C.

2.3. LC-MS analysis of phytochemicals

High-resolution ultra-performance liquid chromatograph mass spectrometry (UPLC-MS) analysis was performed using a Waters Cyclic select IMS quadrupole time-of-flight (QTOF) MS connected to a Waters (UPLC) (Waters, Milford, MA, USA). Electrospray ionisation was used in both negative and positive ion modes, with a cone voltage of 15 V, a desolvation temperature of 275 °C, a desolvation gas flow rate of 650 L/h, and the remaining MS settings optimised for maximum resolution and sensitivity. Data were collected by scanning from 150 to 1500 *m/z* in both resolution and MSE modes. In MSE mode, two channels of MS data were acquired: one at low collision energy (4 V) and the second using a collision energy ramp (40–100 V) to obtain fragmentation data as well. Leucine enkephalin was utilised as the lock mass (reference mass) for precise mass determination, and the device was calibrated with sodium formate. A Waters HSS T3 column (2.1 × 150 mm) was used for separation. The injection volume was 2 µL, with the mobile phase consisting of 0.1 % formic acid in water (solvent A) and acetonitrile containing 0.1 % formic acid (solvent B). The gradient began at 100 % solvent A for 0.5 min and progressed to 100 % B over 12 min in a linear fashion. It then maintained 100 % B for 1 min, followed by a 0.1-minute wash step at 100 % B, before re-equilibrating to initial conditions until the 15th minute. The flow rate was 0.35 mL/min, with the column temperature kept at 55 °C.

MassLynx™ software version 4.1 (Waters, Milford, MA, USA) was used to collect and process data. Data were converted from project files (.PRO) to NetCDF files (CDF) in MassLynx™ using Databridge before being imported into MZmine for analysis. To process the MS data, the following variables were changed: *m/z* tolerance to 0.01 or 10 ppm, and retention time tolerance to 0.1 min. The data matrix was analysed to extract and analyse peak regions for individual ions. The retention time (RT), mass-to-charge ratio (*m/z*), and MS/MS data were combined to forecast new chemicals (Fig. 1).

2.4. Validation of analytical protocols for UHPLC-MS method and quantification of samples using UPLC-QTOF-MS and HPLC-DAD

The developed UHPLC-MS technique was validated using the linearity curve, limit of detection (LOD), limit of quantification (LOQ), precision, and recovery recommendations from the International Conference on Harmonisation (ICH) (Zhao et al., 2020). The standard combination was injected at various concentrations (0.5, 1.0, 2.0, 5.0, and 10.0 ppm) for measurement purposes. The linearity of the calibration curve was tested by plotting the peak areas against a series of standard solution concentrations (mg/L) and evaluating the correlation coefficient with a linear regression model. When $R^2 > 0.99$, the system was always linear. LOD and LOQ were determined using the analytical curve parameters (standard deviation of response and slope).

The repeatability of samples was tested using intraday and interday variations, and the relative standard deviation (RSD) was used to calculate precision. The intraday and inter-day variations were evaluated using six replicates on the same day and three successive days. For each detected peak, the % RSD of peak regions (UV detection) and retention times were calculated. The intraday repeatability (provided as % RSDs) of the RTs ranged from 0.25 to 4.14 %, while the interday repeatability ranged from 1.5 to 3.0 %. The intraday repeatability (provided as % RSDs) of the total peak area was 0.4–0.9 %, while the interday repeatability was 1.5–1.5 %.

The method accuracy was assessed by adding known amounts of standards to samples at three levels: low (50 % of the known amounts), medium (the same as the known amounts), and high (150 % of the known amounts). This procedure was applied in triplicate. The methodologies show that the chemicals were detectable and quantifiable in the extract sampled with high sensitivity, as demonstrated by their limits of quantification and detection (LOQs and LODs, respectively). The observed LODs and LOQs, as well as the predicted recoveries, show that this approach is suitable for profiling chemicals from the samples in the current study (Table 1).

2.5. Cytotoxicity

2.5.1. Cell culture maintenance

The ROS scavenging capacity and AChE inhibition assays were done in vitro, using two cell lines: the genetically modified rat hepatoma cells (H4IIE-*luc* cell line) (Aarts et al., 1993; Jimoh et al., 2024) and the Vero (non-cancerous) cell line, derived from African green monkey kidney cells. The University of Saskatchewan, Saskatoon, Canada, gifted the H4IIE-*luc* cells. It is presumed that the nature of its genetic modification would not impact the cells' behaviour, given that it is focused on expressing a firefly gene in the presence of aryl-hydrocarbon receptor (AhR) ligands and that AhR is endogenous to this cell line. The unmodified Vero cells were obtained from the American Type Culture Collection (ATCC) (Manassas, Virginia, USA) (HB-8065). Both cell lines were cultivated at 37 °C in humidified air supplemented with 5 % CO_2 in Dulbecco's Modified Eagle's Medium (DMEM) (Sigma: D2902; St. Louis, MO, USA) supplemented with 10 % foetal bovine serum (Thermo Scientific, USA) (Idris et al., 2023). All tissue culture work was done aseptically and, where applicable, inside a biosafety cabinet.

2.5.2. Cell viability assay (MTT)

A colorimetric assay measured cell viability based on metabolic activity using the yellow dye 3-(4,5-dimethyltiazol-2yl)-2,5-diphenyl

Table 1
Measures of analytical protocol used in the quantification of phenolic bioactive compounds.

No	Name	t_R (min)	UV_{max} (nm)	(M-H) *m/z* –	MS/MS (*m/z*)	Regression equation	Linear range (mg/L)	R^2	LOD (mg/L)	LOQ (mg/L)
1	Citric acid	1.25	278	191	111	$y = 11023x - 2005$	0.5–10.0	0.999	1.1	3.6
2	Galic acid	3.03	278	169	125	$y = 1553.3x + 938.1$	0.5–10.0	0.998	7.7	25.8
3	Glucose	3.71		161	111	$y = 4091x + 378$	0.5–10.0	0.999	2.9	9.8
4	Neochlorogenic acid	3.61	300, 309	353	191, 179	$y = 29803x + 1930$	0.5–10.0	1.000	0.4	1.3
2	Catechin	3.99	279	289	289, 245, 204	$y = 22713x - 1423$	0.5–10.0	1.000	0.5	1.8
6	Rutin	4.74	254, 255, 354	609	609, 301	$y = 48655x - 4425$	0.5–10.0	0.997	0.2	0.8
7	Pelargonidin 3-rutinoside	5.18	284, 330	579	579, 271	$y = 43767x - 3738$	0.5–10.0	0.997	0.3	0.9
8	Peonidin-3-O-rutinoside	5.29	284	609	609, 299	$y = 28723x + 4124$	0.5–10.0	1.000	0.4	1.4
9	Kaempferol	6.95		285	285	$y = 37364x - 7847$	0.5–10.0	0.997	0.2	0.8

The quantification of compounds has been expressed as citric acid, gallic acid, glucose, neochlorogenic acid, catechin, rutin, pelargonidin 3-rutinoside, peonidin-3 O-rutinoside and kaempferol equivalents. Where t_R = Retention time, M-*H* = Negative ion mode, MS = Mass spectrometry, LOD = Limit of detection, and LOQ = Limit of quantification.

tetrazolium bromide (MTT; Sigma-Aldrich (Pty) Ltd) (Sogoni et al., 2025a). Live cells transform MTT into an insoluble formazan (purple) product using NAD(P)H-dependent cellular oxidoreductase enzymes. A series of six dilutions (0.03, 0.06, 0.13, 0.25, 0.5, and 1 mg/mL) of each plant extract was tested in triplicate in clear 96-well plates. Cells (both Vero and H4IIE-*luc*) were seeded at 80,000 cells/mL and incubated for 24 h before incubation with the respective plant extracts for another 24 h. Each plate had a triplicate of untreated wells (positive control: plant extracts were diluted with cell culture growth medium) as well as untreated wells that were killed with methanol at the end of the exposure period to create a negative control, i.e. all the cells are dead. At the end of the exposure period, the medium was replaced with 500 μg/mL MTT and incubated for 30 min. Purple formazan crystals produced by reduced MTT were dissolved in dimethyl sulphoxide (DMSO), and absorbance was determined spectrophotometrically at 560 nm. The amount of purple formazan produced is associated with the number of viable cells, and the proportion (%) of viable to dead cells was determined by comparing it to the positive control.

Magnitudes of effects of the extracts on cell viability were defined as follows: non-toxic (> 80 %); weakly cytotoxic (60–80 %); moderately cytotoxic (40–60 %); and strongly cytotoxic (< 40 %) (International Organisation for Standardisation (ISO), 2009; López-García et al., 2014).

2.6. AChE activity

2.6.1. Exposure of cells and harvesting cell contents

Non-neuronal AChE is produced in liver cells; therefore, only the H4IIE-*luc* cells were used in this assay. The Ellman assay (Ellman, et al., 1961) was adapted for a 12-well format. This colorimetric assay measures the absorbance of yellow 2-nitro-5-thiobenzoate (TNB) after thiocholine reacts with Ellman's reagent (5,5′-dithio-bis-(2-nitrobenzoic acid); DTNB) (Patel, 2023). The measured absorbance is proportional to AChE activity (Cichon et al., 2025a; Härtl et al., 2011). Cells were seeded at 80,000 cells/mL and exposed to plant extracts at 0.03 mg/mL in triplicate for 24 h after an initial 24 h incubation at 37 °C. Wells with untreated cells were included as controls. The 0.03 mg/mL concentration was the greatest concentration at which none of the samples were cytotoxic to the H4IIE-*luc* cells and was determined in the viability assay (Sub-Section 2.5.2).

The cells were harvested from the 12-well plate by washing with Dulbecco's phosphate-buffered saline (DPBS) and lysing the cells with trypsin. The enzyme activity was stopped with DPBS, and the cell suspension was centrifuged at 1000 *g* for 4 min at room temperature. The supernatant was discarded, and the cell pellet resuspended in 400 μL Tris–HCl/sucrose buffer [12.5 mM Tris–HCl + 125 nM sucrose), vortexed and sonicated at medium intensity for 30 s. This was centrifuged at 10,000 *g* for 10 min at 4 °C. The supernatant was used for AChE inhibitory determination as well as protein content. AChE activity was expressed in terms of the protein content of the cells.

2.6.2. AChE activity assay

This assay was performed in the dark in 96-well white-walled, clear, flat-bottom microplates. Each well received 210 μL ice-cold 0.09 M K_2HPO_4 buffer (pH adjusted to 7.4 by 0.09 M KH_2PO_4), 10 μL each of 30 mM acetylthiocholine iodide and Ellman's reagent (10 mM in methanol). The plates were incubated at 37 °C for 5 min. Sample supernatant was added (10 μL) to the plate in triplicate. Experimental blanks containing the potassium phosphate buffer, acetylthiocholine iodide and Ellman's reagent were included on each plate. Absorbance was measured as soon as possible at 412 nm every minute for six minutes, starting at time zero, resulting in seven points. To determine AChE activity, the mean absorbance of each time interval was determined for the samples, untreated cells, and experimental blanks. This was followed by calculating the reaction gradient. The reaction rate (change in absorbance over six minutes) was determined, and the values were normalised against the protein content. Acetyl choline esterase activity is expressed in absorbance/min/mg/protein (Ellman et al., 1961; Patel, 2023).

2.6.3. Quantification of protein

The total protein concentration in each cell lysate that was harvested after the exposure was determined according to (Bradford, 1976) using bovine serum albumin (BSA) as a standard (0, 62.5, 125, 250, 500, 1000, 2000 μg/mL) (Hanumanthappa et al., 2024). This determination was also performed in the dark in the same plate format as the AChE determination. The standard or the cell lysate (5 μL) was added in triplicate to the wells, followed by 245 μL Bradford's reagent. The protein content was determined by measuring the absorbance at 590 nm in a microplate reader. The protein concentration in the lysate was determined using the regression line formula created by the BSA concentrations and corresponding absorbances.

2.7. Intracellular ROS production and scavenging activity

The 2′,7′-dichlorodihydrofluorescein diacetate (H_2DCF-DA) assay was used to test the intracellular generation of ROS, in the H4IIE-*luc* cells, as well as the scavenging activity of the *T. ciliata* extracts. Intracellular ROS, including hydrogen peroxide (H_2O_2), can be determined using small molecule fluorescent sensors (eg, H_2DCF-DA) that react to

specific stimuli. During the assay, the fluorogenic dye diffuses through the plasma membrane of cells and is hydrolysed to non-fluorescent 2′,7′-dichlorodihydrofluorescein (DCFH) by intracellular enzymes, where it stays trapped (Lebel et al., 1992; Zhang et al., 2021). Under oxidative stress, DCFH reacts with intracellular ROS, leading to the oxidation of DCFH to its highly fluorescent fluorescein derivative, 2′,7′-dichlorofluorescein (DCF) (Engelbrecht et al., 2024). The DCF fluorescence is proportional to the amount of ROS produced.

The method described by Engelbrecht et al. (2024) was applied to determine the AChE activity. Briefly, 80,000 cells/mL H4IIE-*luc* cells were seeded in a 6-well microplate and incubated for 24 h at 37 °C. The cells were exposed to 0.03 mg/mL of *T. ciliata* extract for 24 h in triplicate. A set of three wells received 14.2 ng/mL hydrogen peroxide (H_2O_2) to induce oxidative stress (positive control). The negative control (blank) consisted of cells that had not been treated to H_2O_2 or *T. ciliata* extract. After the 24 h exposure period, the cell medium was replaced with 800 μL 10 μM H_2DCF-DA and incubated for 30 min. The cells were washed, lysed with trypsinand centrifuged at 1 000 g to remove the supernatant. Each cell pellet was resuspended in 800 μL DPBS. The quantification of the fluorescence was measured in black 96-well microplates by transferring 200 μL of the cell suspension into a well (in triplicate for each well on the original 6-well plate resulting in nine fluorescent readings for one sample). Fluorescence was measured as relative fluorescence units (RFUs) at excitation and emission wavelengths of 480 nm and 535 nm, respectively, using a SpectraMax® iD3 multi-mode microplate reader. Since the emitted DCF fluorescence is directly proportional to the amount of ROS produced intracellularly (Engelbrecht et al., 2024; Mattia et al., 1991), the ROS produced by the cells after exposure is calculated based on the difference between the RFUs of treated and untreated cells (blank control).

2.8. Statistical analysis

A one-way analysis of variance was employed to determine the significance of treatment effects. The assumptions of non-parametric statistics were validated. The Mann-Whitney U test was used to determine statistical difference ($p \leq 0.05$) between treated cells and untreated cells using IBM SPSS (version 29.0) statistical software.

3. Results

A total of 71 compounds, grouped into flavonoids, anthocyanins, alkaloids, nucleobase, nucleosides/tide, saccharides, fatty acids, amino acids, and coumarins, were identified in various parts of plants, most of which are known for their vital pharmacological benefits.

3.1. Characterisation of flavonoids

3.1.1. Flavonols

Peak 14 was identified as the flavonoid quercetin-3-O-(6-O-rhamnosylglucoside) (rutin; 3′,4′,5,7-Tetrahydroxy-3-[α-L-rhamnopyranosyl-(1→6)-β-D-glucopyranosyloxy]flavone) (Table 2) (González-Barrio et al., 2018). This is due to conjugation with one or several sugar molecules, as indicated in the fragment ion at *m/z* 447 $[M\text{-}H\text{-}162]^-$. In negative ion mode, fragmentation would produce the aglycone ion of quercetin, with *m/z* of 301. This compound was also identified in positive ion mode (Table 3). Peaks 19 and 20 were identified as kaempferol-3-O-rutinoside and kaempferol-7-neohesperidoside, respectively, after sugar conjugation or malonyl esterification. Upon Collision-Induced Dissociation CID, after losing glucose or any other sugar moiety, parent ions of *m/z* 285 and 284 originating from a hemolytic and heterolytic cleavage of the O-glycosidic bond were observed. This result is consistent with the kaempferol CID spectrum as reported previously (Grabarics et al., 2022; Ye et al., 2005). Peak 23 was identified as isorhamnetin-3-O-rutinoside due to the fragmentation that could lead to isorhamnetin aglycone (315 Da) and ions and UV absorbances consistent with previous reports (Rivera-Pastrana et al., 2010). The fragment ions are at *m/z* 323, 443, and 447.

3.1.2. Flavones

Peaks 21 and 22 were identified as luteolin-6-C-glucoside (isoorientin; 6-(β-D-Glucopyranosyl)-3′,4′,5,7-tetrahydroxyflavone) and luteolin-8-glucoside (homoorientin; Isoorientin; 6-(β-D-Glucopyranosyl)-3′,4′,5,7-tetrahydroxyflavone), respectively. The UHPLC-TOF/MS in the negative ion mode of peak 16 had a molecular ion $[M\text{-}H]^-$ of *m/z* 609.1479 and fragment ions at *m/z* 327. The fragment ions at *m/z* 327 $[(M\text{-}H)\text{-}(90{+}30{+}162)]^-$ were typically characterised as the *C*-glycosylflavone group, based on a previous literature (Lee et al., 2016). Moreover, this ion *m/z* 327.0515 was formed by mono glycosylflavone with the loss of 120 amu. Accordingly, the fragment ion fragmentation pattern is characteristic of luteolin. Therefore, this peak was elucidated as luteolin-6,8-di-*C*-glucoside (lutonarin) (Ferreres et al., 2008; Lee et al., 2016). Luteolin-3′,7-di-O-glucoside (peak 59) was identified at RT of 4.30 in the negative ion mode from databases (MassBank, ResPect).

3.1.3. Flavanones

Chromatographic peak 16 generated fragment ions at *m/z* 243 $[M\text{-}H\text{-}CO]^-$ and 227 $[M\text{-}H\text{-}CO_2]^-$and was identified as 3′,4′,7-trihydroxyflavanone, which is a flavanone (Shen et al., 2017). It Apigenin-6-C-glucoside-7-O-glucoside was eluted at RT 4.64 min and exhibited the characteristic ion *m/z* 271 of the apigenin aglycone.

3.2. Identification of anthocyanins

Anthocyanins are a group of O-glycosides of 3,5,7,3-tetrahydroxyflavylium cation responsible for the red, blue, and violet colors of most berries and other fruits and vegetables. The two anthocyanin monoglycosides (*m/z* 449 and 433) produced their corresponding aglycones (cyanidin and pelargonidin) like peonidin-3-O-beta-galactopyranoside with the aglycone cation (*m/z* 271) and a fragment at *m/z* 595 during product-ion analysis which matched previously reported. Peak 33 represented peonidin aglycone with 279, 284, and 265. The desugar conjugates, such as cyanidin-3-O-(2′'-O-beta-glucopyranosyl-beta-glucopyranoside), cyanidin-3-O-rutinoside,delphinidin-3-O-(6′'-O-alpha-rhamnopyranosyl-beta-glucopyranoside) and correspond to loss of rhamnose from the molecular cation.

3.3. Identification of alkaloids, nucleobase, nucleosides/tide

Peak 28 was tentatively identified as N-trans-coumaroyl-tyramine in both positive and negative ion modes. It had a molecular ion $[M\text{-}H]^-$ at *m/z* 282 and major MS^2 fragments *m/z* 119 ([coumaric acid-CO_2]$^-$ and *m/z* 173 [M-H- coumaric acid-CO_2]$^-$(*p*-coumaric acid; (2*E*)-3-(4-Hydroxyphenyl)prop-2-enoic acid). Compound 29 was identified as N-trans-feruloyl-tyramine ((*E*)-3-(4-hydroxy-3-methoxyphenyl)-*N*-[2-(4-hydroxyphenyl)ethyl]prop-2-enamide) with $[M\text{-}H]^-$ ion at *m/z* 312 and *m/z* 173 [M-2H- tyramine]$^-$, 145 [M-H- tyramine-2CH_3]$^-$. Compounds showed an $[M + H]^+$ ion at *m/z* 188 with the same formula, $C_{11}H_9O_2N$. The fragment ions at *m/z* 170 $[M + H{-}H_2O]^+$, 143 $[M + H{-}COOH]^+$, 118 $[M + H{-}C_2H_2COOH]^+$, and 91 $[M + H{-}C_4H_5COOH]^+$ were produced in the MS^2 spectrum. They were tentatively identified as trans-3-indoleacrylic acid and indole-3-acrylic acid, respectively generated an $[M + H]^+$ ion at *m/z* 247.1434, and it further produced fragment ions at *m/z* 188.0701 $[M + H{-}NCH_3]^+$ and 146.0598 $[M + H{-}NCH_3{-}CO_2]^+$. It was unambiguously identified as hypaphorine (αS)-α-carboxy-N,N,N-trimethyl-1H-indole-3-ethanaminium) (Zhang et al., 2011). In addition, N-palmitoyl-D-erythro-sphingosine fatty acid derivative was identified in positive ion mode.

Additionally, nucleoside; adenosine (53, *m/z* 268.1054 $[M + H]^+$) was identified alongside purine nucleobase; adenine ion *m/z* 136 was identified along with its respective. Likewise, pyrimidine nucleoside cytidine (63, *m/z* 242.12854 $[M + H]^+$). The nucleoside fragmentation

Table 2
Analysis of compounds in the negative ion mode.

No	RT	Precursor ion M-H]-	MS/MS	Annotation	Database	Amount in the sample (mg/L)												
						RC	RT1	RT2	RT3	RT4	FC	FT1	FT2	LC	LT1	LT2	LT3	LT4
1	1.59	341.1082	313, 159, 133	Sucrose	MassBank	57.4						47.8					6.3	
2	1.64	341.1086	133	Sucrose Isomer I	ResPect						78.4	47.8						
3	1.64	341.1078	179, 133	D-(+)-Trehalose	ResPect		91.9	63.9	94.3	44.7			65.8	65.8				
4	1.79	191.0193	111	Isocitric acid	ResPect													
5	2.88	341.1081	133	Sucrose isomer II	MassBank, ResPect	14.1				14.8			17.4	14.0	1.0	14.6	13.7	13.9
6	2.88	341.1086	179, 133	D- (+)-Trehalose Isomer I	MassBank		17.2	17.4	13.9		14.8	14.0	17.4	17.4				
7	2.93	191.0185	111, 139	Citric acid/Citrate	MassBank, ResPect	7.2	5.5	3.8	3.1	3.7	10.1	7.6	7.4	10.3	10.4	7.4		4.2
8	2.93	191.0182	111	DL-Isocitric acid	ResPect										6.8			
9	2.93	191.019	111, 128	Scopoletin	ResPect								–	–		–		
10	3.04	282.0852	267	Guanosine	MassBank											–		
11	3.29	173.0075	147	Cis-Aconitic acid	ResPect											2.0		
12	3.34	205.0346	173, 147, 111	DL-6,8-Thioctic acid	MassBank, ResPect						1.4		1.6	3.0	3.0	2.1		
13	3.97	341.0876	179, 203, 323	D-(+)-Trehalose isomer II	MassBank							10.0						
14	4.33	609.1479	447, 327	Rutin	ResPect										0.9			0.4
15	4.33	609.1461	298, 489, 327	Delphinidin-3-O-(6″-O-Alpha-rhamnopyranosyl-beta-glucopyranoside)	MassBank						1.4	0.6	0.8	0.8		0.6	0.6	
16	4.33	609.1479	447, 327	Luteolin-6,8-di-C-glucoside	MassBank								1.5	0.9	0.9			0.4
17	4.58	229.0086		D-Ribose 5-phosphate	MassBank				5.2									
18	4.62	593.1541	473, 298, 357	Keracyanin (cyanidin-3-O-rutinoside)	MassBank, ResPect						4.6						2.2	1.9
19	4.62	593.1514	473, 298	Kaempferol-3-O-rutinoside	MassBank, ResPect								1.5	3.1	3.1		2.0	
20	4.62	593.1514	473, 298	Kaempferol-7-neohesperidoside	ResPect										3.5	1.9		
21	4.72	447.0941	329, 215	Luteolin-6-C-glucoside (isoorientin)	MassBank, ResPect						–		–	–		–	–	–
22	4.72	447.0931	329	Homoorientin	MassBank, ResPect							–		–	–			
23	4.87	623.1618	323, 443, 447	Isorhamnetin-3-O-rutinoside	MassBank, ResPect						0.5		0.4	0.4				
24	5.23	173.0811	147	Suberic acid	MassBank, ResPect				2.0	2.0		2.2	1.8	2.1	2.1	1.9	2.11	1.8
25	5.13	533.0900	489								–							
26	5.91	461.1075	187, 209	Peonidin-3-O-beta-galactopyranoside	MassBank		0.5											
27	5.91	461.1082	187, 209	Peonidine-3-O-glucoside chloride	MassBank			0.5	0.7									
28	6.33	282.1125	187	N-trans-coumaroyl-tyramine	MassBank, ResPect			–										
29	6.42	312.1232	297	N-trans-feruloyl-tyramine	MassBank, ResPect			–										
30	7.28	431.2224	329, 311, 325, 298	Apigenin-8-C-glucoside	MassBank, ResPect													
31	7.53	431.2292	325, 311, 339, 297	Apigenin-6-C-glucoside	MassBank, ResPect													
32	7.91	299.0557	279, 284, 265	Kaempferide	MassBank, ResPect	1.0	1.5	1.3	1.4									
33	7.96	299.0541	279, 284, 265	Peonidin						1.4								
34	7.96	299.0553	265, 297	3 5 7-trihydroxy-4′-methoxyflavone	MassBank	1.0		1.3	1.4									

(*continued on next page*)

Table 2 (*continued*)

No	RT	Precursor ion M-H]-	MS/MS	Annotation	Database	Amount in the sample (mg/L)										
						RC	RT1	RT2	RT3	RT4	FC	FT1	FT2	LC	LT1	LT2	LT3	LT4
35	9.22	343.2128		17-HDoHE	ResPect		–								–	–	–	
36	11.51	311.2004	293, 265, 211	Dihydroxyoctadecadi-enoic acid	MassBank													
37	11.71	311.2007	183, 211	Methyl-13-hydroperoxy-delta9Z,11E-octadeca-dienoic acid	ResPect		–					–						
38	12.26	341.1126	325	Melibiose	MassBank								36.0			31.0		
39	12.26	341.1098	325	Gentiobiose	ResPect					25.2								
40	12.31	341.1094	325	Sucrose isomer III	MassBank					25.6			36.1	36.0	29.8	31.0		
41	13.11	293.1773	265	Hydroxylinolenic acid	ResPect													
42	13.45	149.9916		Benzisothiazolone (BIT)	MassBank, ResPect	–	–					–	–	–	–	–	–	–
43	13.99	506.3192		Phosphatidylethano-lamine lyso 20	MassBank	–	–											
44	14.06	806.63		Phosphatidylethanolamine alkenyl 18	ResPect													–
45	14.06	423.2309		Pravastatin	ResPect											–		
46	14.25	455.1045		Riboflavin-5′-monophos-phate	ResPect							–						–
47	14.30	341.1082	325	Melibiose isomer I	ResPect								92.7					
48	14.25	341.1104	179, 325	D-(+)-Trehalose isomer IV	MassBank				98.7	98.7						82.3		108.0
49	14.30	341.1079	179, 325	D-(+)-Trehalose isomer V	MassBank, ResPect	83.1	89.5	118.0	98.7	85.9	90.0	85.6	17.4	167.4	167.4	82.3	83.6	109.0
50	14.30	455.101		Riboflavin-5′-mono-phoshate isomer	MassBank, ResPect	–	–	–	–	–	–	–	–	–	–	–	–	–

For sample codes RC=1= Root Control, RT1=2=Root T1, RT2=3=Root T2, RT3=4=Root T3, RT4=5=Root T4, FC=6= Flower Control, FTI=7=Flower T1, FT2=8=Flower T2, LC=9=Leaves control, LT1=10=Leaves T1, LT2=11=Leaves T2, LT3=12=Leaves T3, LT4=13=Leaves T4. Dash means identified but not quantified due to the absence of a standard.

Table 3
Analysis of compounds in the positive ion mode.

No	RT	Precursor ion $[M+H]^+$	MS/MS	Metabolite name	Sample
51	2.94	325.1135	185, 137	P-Coumaric acid glucoside	RC, RT1,
52	2.94	224.1295		Cerulenin	RC, RT1, LTI, LT2, LT3, LT4
53	2.94	268.1054	152, 136, 204, 231	Adenosine	LTI, LT2,
54	3.10	247.1678	124, 142	Hypaphorine	
55	3.30	229.0333		Not identified	
56	3.39	120.0847		Not identified	
57	3.40	166.0890	120,103	L-(-)-Phenylalanine	LTI, LT2, LT3, LT4
58	3.41	395.1344	188	Hypaphorine	RC, LT1
59	4.30	611.1634	499, 299	Luteolin-3′, 7-di-O-glucoside	LT1
14	4.34	611.1625	303	Rutin	LT2
19	4.63	595.1668	287	Kaempferol-3-O-rutinoside	LT2, LT3, LT4
60	4.64	595.1674	271	Apigenin-6-C-glucoside −7-O-glucoside	LT1
21	4.74	449.1095	287	Luteolin-6-C-glucoside	LTI, LT2, LT4
28	6.33	284.1125	187	N-trans-coumaroyl-tyramine	RC, RT1
29	6.42	314.1232	297	N-trans-feruloyl-tyramine	RC, RT1, RT2, RT3, RT4, FC, FT1, FT2, LC, LT1
61	6.74	219.1759	147	Ethoxy-methoxycoumarin	RC
62	7.66	219.1756	147	Ethoxy-methoxycoumarin isomer	RC
63	7.98	242.2854	112	Cytidine	RC, RT1, RT2, RT3, RT4, FC, FT1, FT2, LC, LT1
64	8.44	281.2484^K	275	Linoleic acid	
65	11.58	149.0264		Citramalate	LT2
66	12.42	223.2074		Alpha-Bisabolol	LT3
67	12.45	223.2069	207, 73	Farnesol (mixture of isomers)	RC, RT1, LT4
68	12.77	149.0267	149	Citramalate isomer	RC, RT1, LTI, LT2, LT3, LT4
69	12.77	398.2331	149	Citramalate isomer II	RC, RT1, LTI, LT2, LT3, LT4
70	12.90	538.5190	264	N-Palmitoyl-D-erythro-Sphingosine	RC
71	13.5	393.3014		Sodium deoxycholate	RT1, LTI, LT2, LT3, LT4

Sample codes: RC= Root Control, RT1=Root T1, RT2=Root T2, RT3=Root T3, RT4=Root T4, FC= Flower Control, FTI=Flower T1, FT2=Flower T2, LC=Leaves control, LT1=Leaves T1, LT2=Leaves T2, LT3=Leaves T3, LT4=Leaves T4. Note: The quantification was done in negative mode since standards, and many compounds were better analysed in the negative mode.

pattern involved the cleavage of the glycosidic linkage to give the respective nucleobase at *m/z* 136 (adenine) and 112 (cytosine).

3.4. Identification of saccharides

Non-reducing disaccharides: sucrose and its isomers (1,2,5,40), and trehalose and its isomers (3, 6, 13, 48, 49), melibiose (38, 47) and

gentiobose (39), were differentiated through their elution time, and accurate masses. Reducing ones which displayed *m/z* 341 $[M\text{-}H]^-$ and produced *m/z* 179 as the base peak by glycosidic link cleavage (Calvano et al., 2017). The neutral loss of one and two hexose units through oxygen linkages was observed at *m/z* 325: The ion 179 and 161 due to loss of water.

3.5. Identification of fatty acids

Peaks 36, 37, 41 and 64 were identified as polyunsaturated and hydroxylated fatty acids. Peak 64 was identified as linoleic acid. Its fragmentation pattern is similar to previous work by Serag et al. (2019a). Its hydroxylated form was represented at peak 41. Linoleic acid

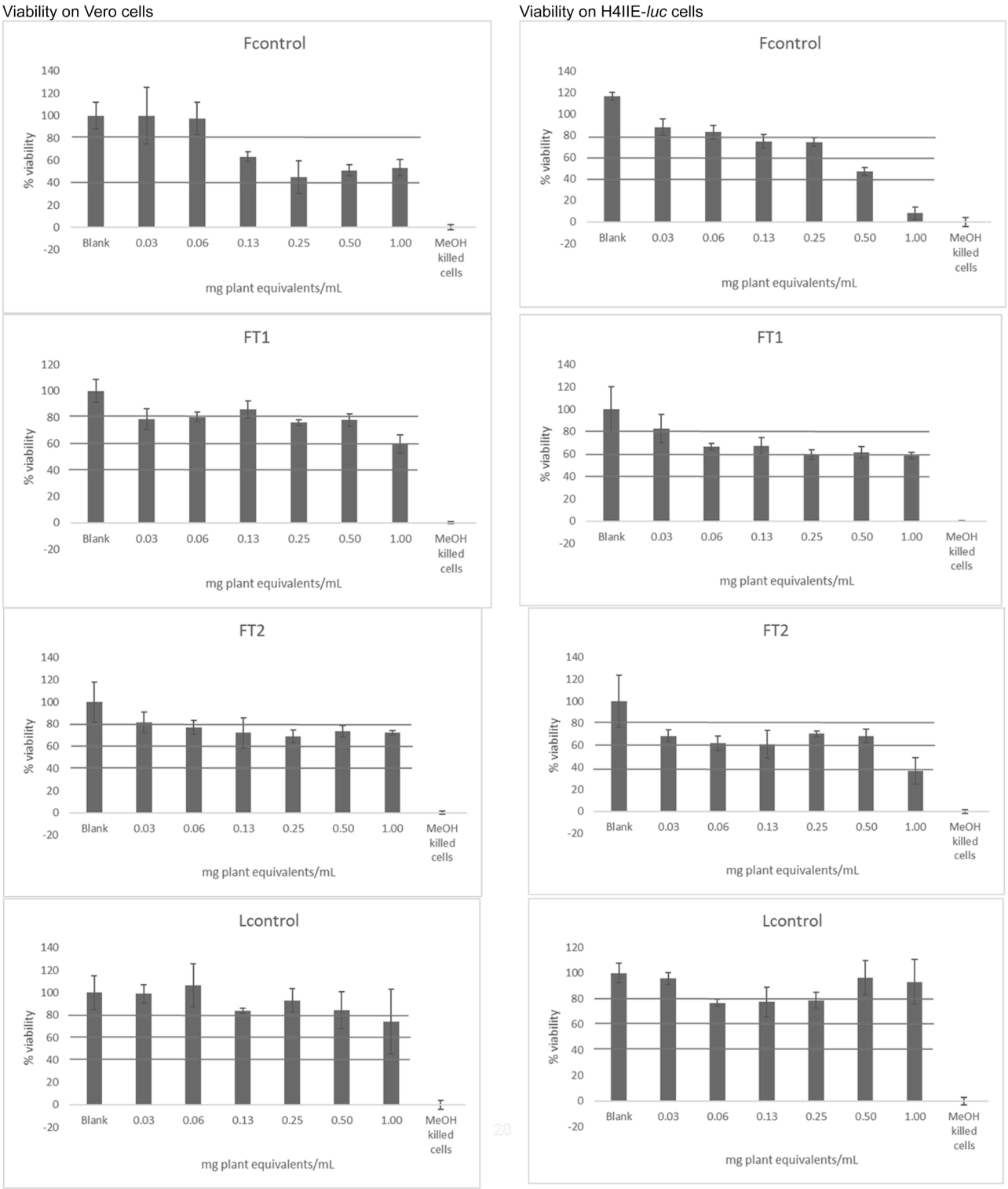

Fig. 2. Cytotoxicity of the different concentrations of *T. ciliata,* Flower buds (F), Leaves (L) and Root (R) extracts in mg/mL against H4lIE-*luc* and Vero cells. Blank represents positive control (untreated cells). *F* = flower bud extracts, *L* = Leaf extract, and *R* = root extracts. Control = 0 mM NaCl, T1= 50 mM NaCl, T2 = 100 mM NaCl, T3 = 150 mM NaCl, T4 = 200 mM NaCl. Cell viability: > 80 % = non-cytotoxic, 60–80 %= weak cytotoxicity, 40–60 % = moderate cytotoxicity, < 40 %= strong cytotoxicity.

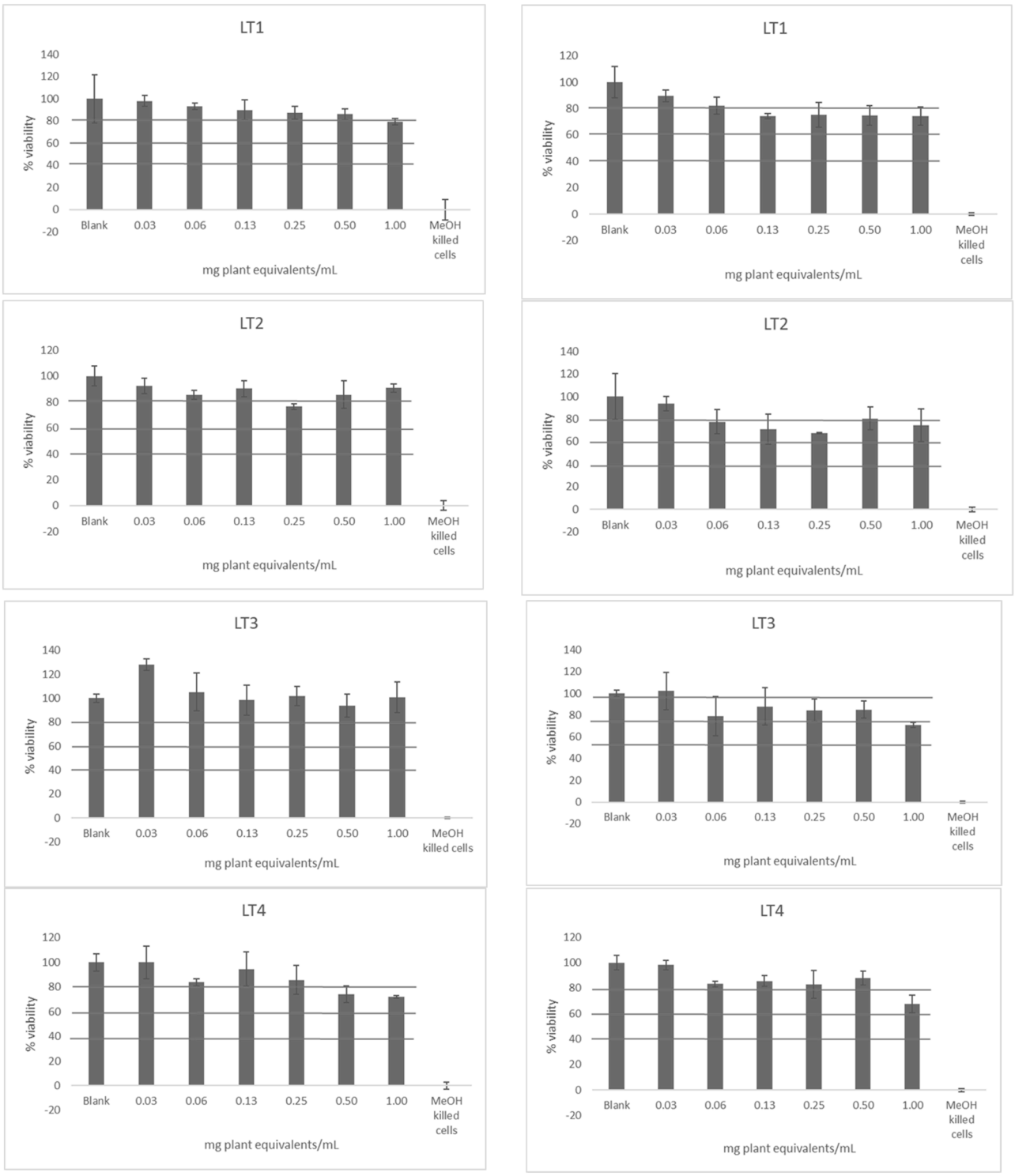

Fig. 2. (*continued*).

is an essential fatty acid that possesses anti-inflammatory properties by providing the building blocks for prostaglandins. Several other hydroxylated fatty acids were also detected as major peaks, and they showed an extra loss of water molecules (Serag et al., 2019b). The polyunsaturated fatty acids included dihydroxy-octadecadienoic acid and methyl-13-hydroperoxy-delta9Z,11E-octadecadienoic acid. Dihydroxy-octadecadienoic acid showed main MS/MS fragments at *m/z* 311 and 293 due to the subsequent loss of two water molecules and the main fragment at *m/z* 211 due to the C15\ C16 bond cleavage (MassBank, ResPect) (Serag et al., 2019a).

3.6. Identification of organic and carboxylic acids

There were eight carboxylic acids identified in the extract, namely citric acid (7), isocitric acid (8), 2-isopropylmalic acid (4), cis-aconitic acid (11), 6,8-thioctic acid (12) and suberic acid (24). Fragmentation of the carboxylic acids occurred mostly by releasing one or two H_2O molecules, which are characterised by the ion fragments $[M\text{-}H\text{-}18]^-$ and

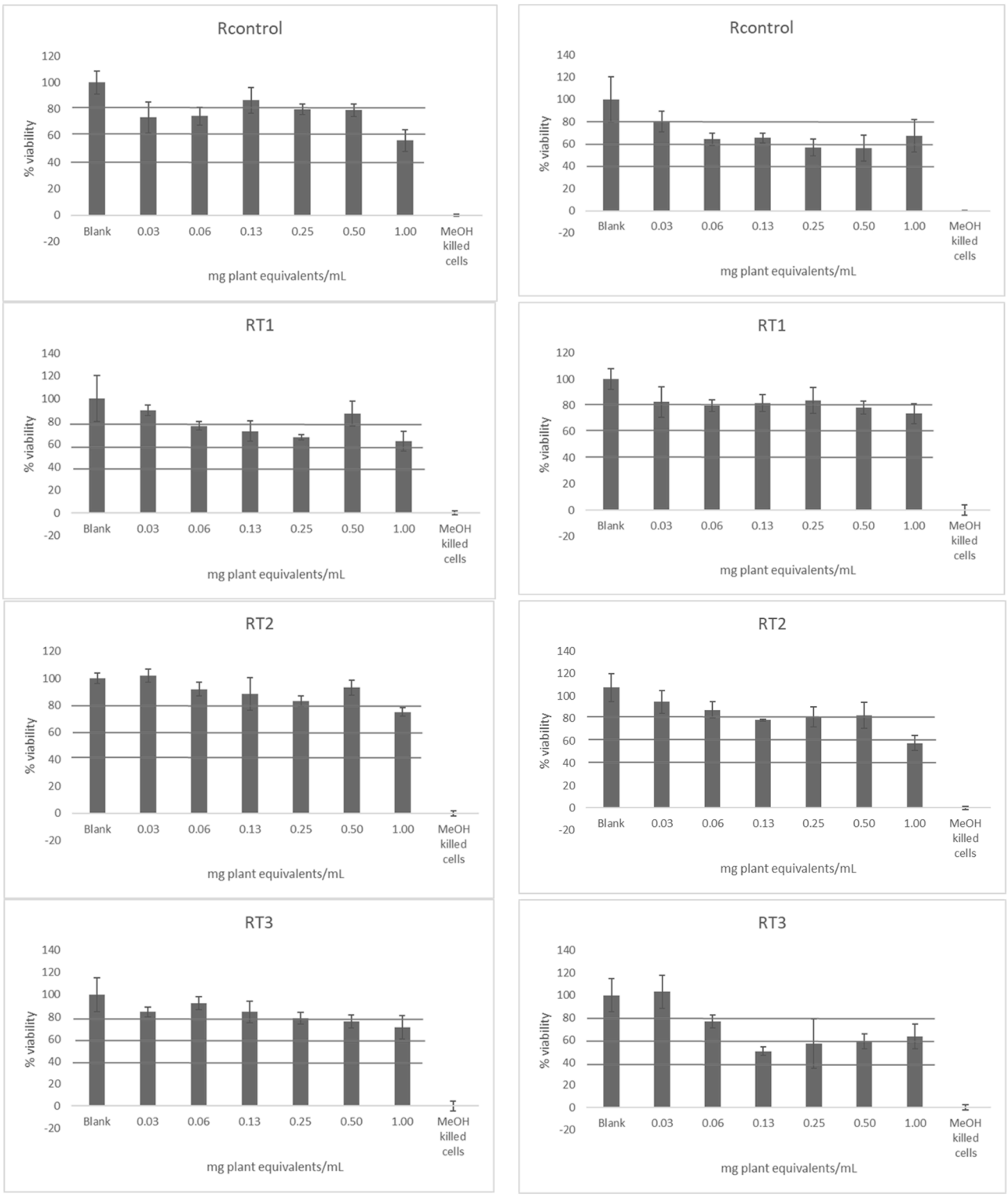

Fig. 2. (*continued*).

CO_2, at *m/z* 129 $[M\text{-}H\text{-}CO_2]^-$ and 111 $[M\text{-}H\text{-}CO_2\text{—}H_2O]^-$ for trans-aconitic acid and citric acid.

3.7. Identification of coumarins

Coumarins were detected at peaks 9, 61 and 62, most of which exhibited characteristic UV λ_{max} at about 274 nm. Peak 1 belonged to a dihydroxyl derivative of coumarin through the addition of more of the 16 mass units to *m/z* 147 for coumarin. Free coumarin was identified at peak 2 with characteristic MS/MS fragment ion, *m/z* 103 after retro Diels Alder cleavage through the lactone ring of coumarin. Peak 9 was tentatively identified as scopoletin via its lithium adduct in the positive ion mode with MS^2 of characteristic ion, *m/z* 191 $[M\text{-}H]^-$. Peaks 61 and 62 were identified as ethoxy-methoxy coumarin derivatives after adding methoxy or ethoxy units of 31 or 45, respectively on coumarin, *m/z* 147.

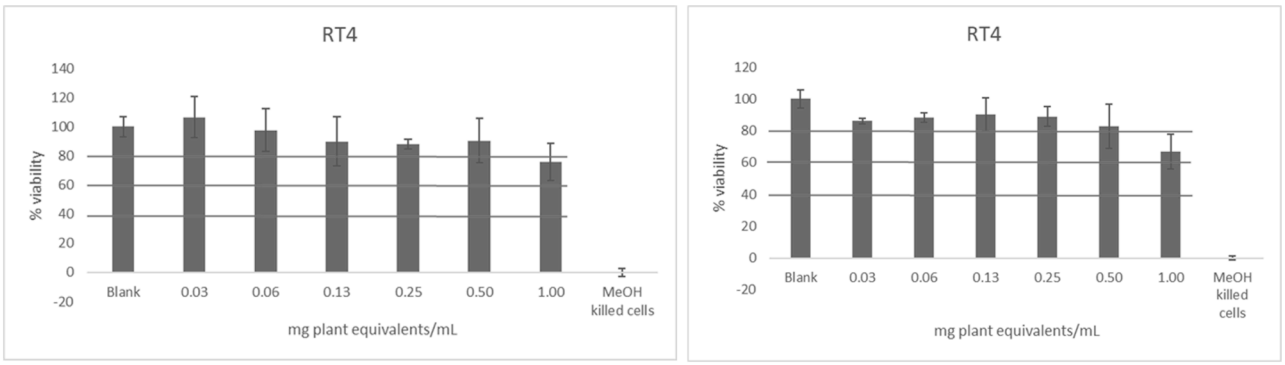

Fig. 2. (*continued*).

3.8. In vitro cytotoxicity determination

Ethanolic extracts of flower buds, leaves, and roots of *T. ciliata* cultivated under different salinity treatments significantly influenced cell viability of rat hepatoma (H4IIE-*luc*) and African green monkey kidney (Vero) cells (Fig. 2). Flower bud extracts prepared from 0 mM and 100 mM salinity treatments at 1 mg/mL extract concentration showed strong cytotoxicity (< 40 %) to H4IIE-*luc*, while they had moderate and weak cytotoxicity to Vero cells, respectively. Root extract obtained from 0 mM salinity treatment at 0.5 mg/mL extract concentration showed moderate toxicity to H4IIE-*luc* cells, while it was non-cytotoxic (> 80 %) to non-cancer cells. Moreover, root extract prepared from 150 mM salinity treatment at 0.13 mg/mL showed moderate cytotoxicity to H4IIE-*luc* cells, while it was not cytotoxic to Vero cells. All other extracts showed mild cytotoxicity to both cancer and non-cancer cells.

Fig. 3

3.9. AChE activity

All ethanolic extracts of *T. ciliata* exhibited anti-AChE activity. The highest AChE inhibitory activity was observed from the cells treated with extract from flower buds at 100 mM salinity concentration, followed by root extract obtained from 100 mM salinity concentration. The lowest activity was exhibited by leaves cultivated under 150 mM salinity treatment.

3.10. Intracellular ROS scavenging activity

Based on the results of the 7′-dichlorodihydrofluorescein diacetate assay (H_2DCF-DA) in vitro *T. ciliata* extracts leaf, root, and flower bud of *T. ciliata* cultivated under varying salinity treatments notably influenced the intracellular production of ROS compared to the untreated cells (Fig. 4). The cells that received the peroxide had a surprisingly low production of ROS. The highest significant ROS scavenging activity was observed in the cells treated with extracts prepared from roots at 0 mM salinity treatment. All leaf extracts showed ROS scavenging activity. The ROS scavenging activity of leaf extracts was indirectly proportional to increasing salinity concentration.

4. Discussion

Despite the current surge in interest worldwide in the therapeutic potential of medicinal halophytes, South African halophytes have

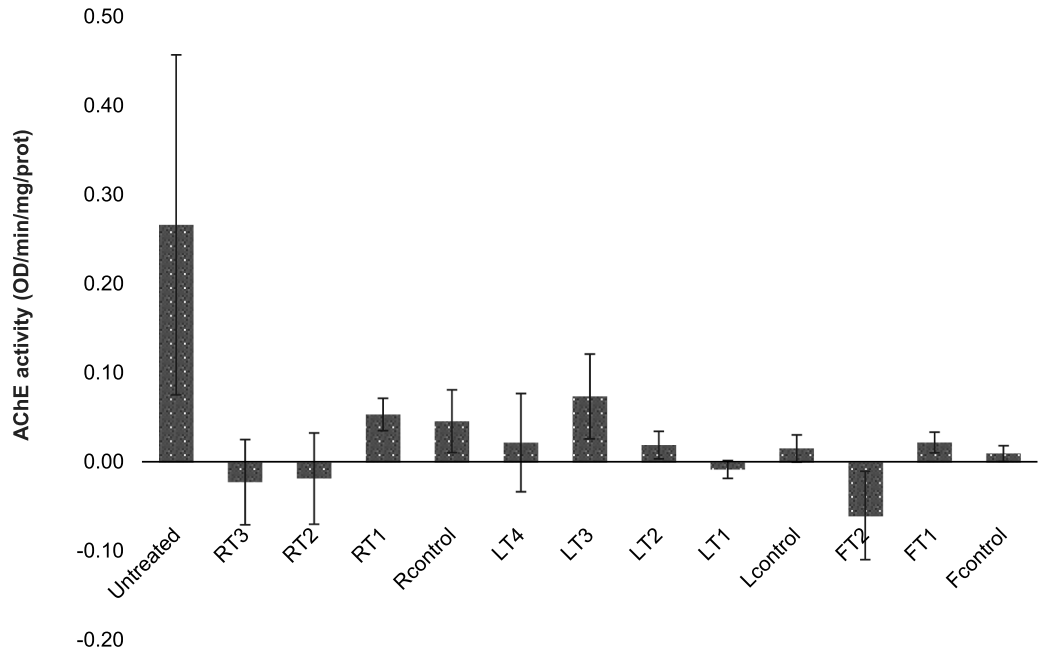

Fig. 3. AChE activity of the plant extracts (OD/min/mg/prot) compared to the control (untreated cells). *F* = flower buds extracts, *L* = Leaf extract, and *R* = root extracts. Control = 0 mM NaCl, T1 = 50 mM NaCl, T2 = 100 mM NaCl, T3 = 150 mM NaCl, T4 = 200 mM NaCl.

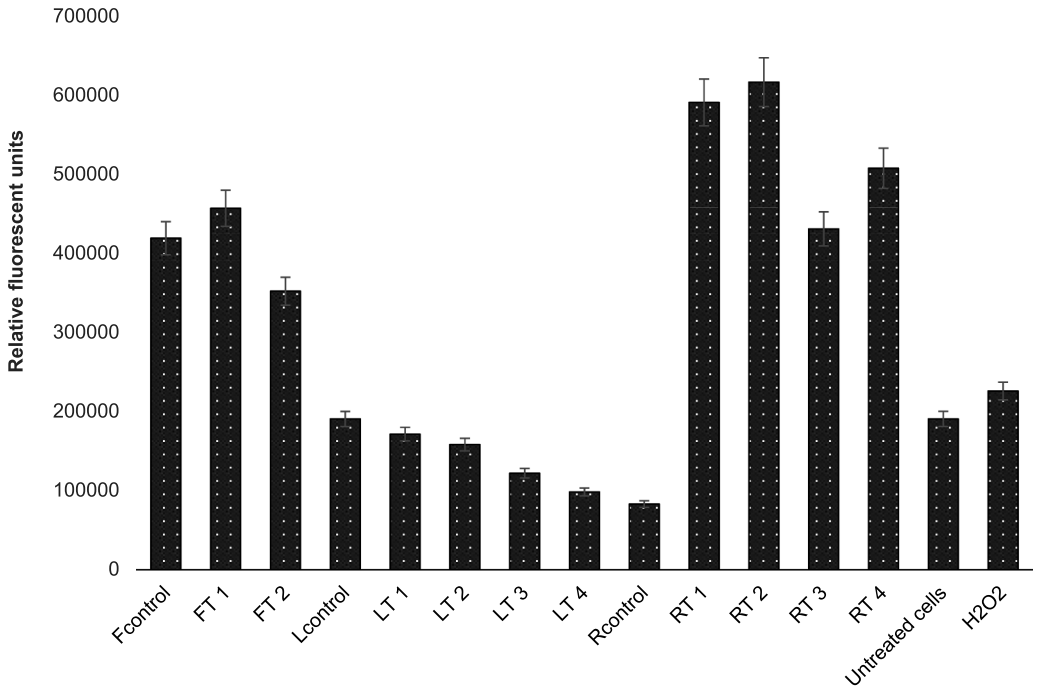

Fig. 4. Reactive oxygen species production in liver epithelial hepatoma H4IIE-*luc* cells. Data are expressed as mean ± standard deviation. *F* = flower buds extracts, *L* = Leaf extract, and *R* = root extracts. Control = 0 mM NaCI, T1 = 50 mM NaCl, T2 = 100 mM NaCl, T3 = 150 mM NaCl, T4 = 200 mM NaCl, H2O2 = H_2O_2.

received little attention as possible agents for the treatment of chronic illnesses (Cock, 2015; Sogoni et al., 2025b). *Trachyandra ciliata* is one of the understudied, wild, edible halophytes from South Africa (Ngxabi et al., 2024). A previous study by Ngxabi et al. (2025) validated its edibility and reported that salinity improved its nutritional composition and antioxidant capacity. However, the pharmacological potential of the species remained undocumented. Thus, the present study investigated the crude extracts of *T. ciliata* as a potential therapeutic agent for the treatment of prominent chronic diseases such as cancer, cognitive impairment, and ROS production in the liver. In the current study, the UHPLC-MS phytochemical profiling of different parts of *T. ciliata* identified 71 compounds grouped into flavonoids, anthocyanins, alkaloids, nucleobase, nucleosides/tide, saccharides, fatty acids, amino acids, and coumarins, most of which are known for their vital pharmacological benefits.

Cancer remains a significant global health issue, accounting for the second highest cause of deaths in the current millennium (Mohammed et al., 2023; Siegel et al., 2019; Zafar et al., 2025). Due to complications associated with conventional cancer treatments, plant-based approaches are gaining popularity because they offer a potential complementary or alternative option at a lower price and reduced side effects (Ferreira et al., 2022; Lee et al., 2024; Sogoni et al., 2025a; Venkatachalapathy et al., 2021). In the present study, ethanolic extracts of flower buds, leaves, and roots of *T. ciliata* cultivated under different salinity treatments significantly influenced the cell viability of cancer and non-cancer cells. Flower bud extracts prepared from 0 mM and 100 mM salinity treatments at 1 mg/mL concentration showed strong cytotoxicity to cancerous cells, while they had moderate and weak cytotoxicity to non-cancerous cells, respectively. Root extract obtained from 0 mM salinity treatment at 0.5 mg/mL extract concentration showed moderate toxicity to H4IIE-*luc* cells, while it was non-cytotoxic to non-cancerous cells. The anti-cancer activity of the extracts of *T ciliata* can be attributed to the presence of anti-cancer compounds such as quercetin-3–0-(6–0-rhamnosyglucoside), isor hamnetin-3-O-rutinoside, luteolin, and scopololetin that were identified by the UHPLC-MS as shown in Tables 2 and 3. These compounds have been widely reported in literature as anticancer metabolites (Gong et al., 2020; Jiang et al., 2022; Jimoh et al., 2024). Luteolin for instance has been shown to have biological actions against cancer, such as promoting apoptosis in lung cancer cells, inhibiting tumour proliferation, invasion, and metastasis, modulating immune responses, and acting as an adjuvant to radio chemotherapy (Çetinkaya and Baran, 2023; Zhang and Ma, 2024). A study by Meilawati et al. (2023) reported that scopoletin inhibited the proliferation in LNCaP prostate cancer cells in a dose-dependent manner, and it caused G2/M phase growth halt and an increase in the sub-G0/G1 cell population after treatment with increasing doses, resulting in cell death. Furthermore, it was reported that plant-derived isorhamnetin-3-O-rutinoside inhibited tumour expansion by increasing cleaved caspase-9, Hdac11, and Bai1 protein levels in xenografted immunosuppressed mice (Antunes-Ricardo et al., 2021; Wang et al., 2023). Alternatively, quercetin has been used over the years as a chemoprevention drug in numerous forms of cancer because of its antioxidant, anti-tumour, and anti-inflammatory properties (Boretti, 2023; Jeong et al., 2009). Asgharian et al. (2022) reported that quercetin possesses anti-cancer characteristics that reduce tumour proliferation, invasion, and metastasis while also modulating the activity of oncogenic and tumour suppressor ncRNAs. The presence of these biological compounds in the extracts of *T. ciliata* suggest that it has a potential as a therapeutic agent in the treatment of cancer, although further isolation of these compounds is recommended for future studies.

Alzheimer's disease (AD), the most prevalent neurodegenerative disorder and the cause of adult-onset cognitive impairment, is distinguished by a gradual loss of cognitive abilities accompanied by behavioural symptoms (Marucci et al., 2021). An increase in AChE plays an important role in acetylcholine (ACh) depletion, leading to Alzheimer's disease (Huang et al., 2022). Thus, acetylcholinesterase inhibitors (AChEIs) have been used as the main treatment for AD (Gajendra et al., 2024; Kaushik et al., 2018). Plant-based compounds, including halophytes have begun to gain recognition globally as promising acetylcholinesterase inhibitors because of the side effects associated with synthetic drugs (ALNasser et al., 2025; Islam et al., 2024; Taqui et al., 2022).

Results from the present study revealed that ethanolic extracts of leaves, roots, and flower buds of *T. ciliata* had high AChE inhibitory activity compared to untreated cells. The highest AChE inhibitory

activity was observed from the cells treated with extract from flower buds at 100 mM salinity concentration, followed by root extract obtained from 100 mM salinity concentration. The UHPLC-MS identified numerous phytochemicals in the crude extracts of *T. ciliata* that are linked to activities against neurodegenerative disorders such as quercetin and kaempferol (flavonols), peonidin (anthocyanins), tyramine (alkaloid), trehalose (disaccharide), linoleic acid (fatty acid), and scopoletin (coumarin), have all been linked with amelioration of neurodegenerative disorders (Abuzaid et al., 2020; Song et al., 2022). The high AChE inhibitory activity of *T. ciliata* extracts observed in this study can be directly attributed to the presence of these biological compounds. Flavonols such as quercetin and kaempferol have been reported to exhibit potent inhibition of acetylcholinesterase in previous studies. Recent studies have reported that plant-derived kaempferol demonstrates strong suppression of AChE based on the presence and location of the hydroxyl groups (Adetuyi et al., 2024a; Cichon et al., 2025). Other studies suggest that it also increases acetylcholine (ACh) levels in the brain, improves memory function, and mitigates cognitive deficits, suggesting that kaempferol may be useful as a treatment for AD (Adetuyi et al., 2024a; Kouhestani et al., 2018; Lin et al., 2023). On the other hand, studies have demonstrated quercetin inhibition of AChE by binding the enzyme through hydrogen bonding, by inducing allosterism, and by reducing Aβ-amyloid deposition, thereby disrupting the enzyme's hydrogen bond setup (Cichon et al., 2025b; Liao et al., 2022; Orhan, 2020). Research has shown that peonidin exhibits AChE inhibitory activity due to its antioxidant activity (Zavala-Ocampo et al., 2022). Tyramine (alkaloid) derived from the bark *Celtis chinensis* in vitro demonstrated AChE inhibitory activity in a dose-dependent manner (Kim and Lee, 2003), which is consistent with recent reports on the AChE inhibition of tyramine (Touhtouh et al., 2025). Moreover, other compounds such as trehalose, linoleic acid, and scopoletin have also been reported to exhibit neurogenerative functions and improve cognitive function (Akay et al., 2023; Karunakaran et al., 2022; Pupyshev et al., 2024). These findings infer that *T. ciliata* could be a potential therapeutic agent in the treatment of AD and other neurodegenerative disorders.

Liver disorders are often associated with excessive production of reactive oxygen species (ROS), which can cause oxidative stress and damage to liver cells, proteins and DNA (Lee et al., 2022). It is therefore important to maintain redox homeostasis to prevent and treat liver disorders (Bellanti et al., 2025; Liu et al., 2023). In the present study, the leaf extracts from all treatments, and the root extract from the 0 mM salinity treatment had high ROS scavenging activity. This activity may be attributed to phytochemicals such as apigenin (flavanone), peonidin (anthocyanin), adenosine (nucleoside), thioctic acid (carboxylic acid), scopoletin (coumarin), which have been reported to reduce oxidative stress in human cells and ameliorate liver disorders (Gao et al., 2024; Tan et al., 2020; Viana et al., 2022; Yoshizane et al., 2020). These compounds were identified in *T. ciliata* extracts (Tables 2 and 3) and are consistent with the findings of Ejiofor et al. (2022) who reported that leaf extracts of *Amaranthus hybridus* (a semi-halophyte) ameliorated oxidative stress and liver damage caused by thioacetamide. Another recent study revealed that *Echinops* species extract reduced oxidative stress, inflammation, and cell death to prevent liver damage induced by malathion (Eid et al., 2024). This suggests that phytochemicals from *T. ciliata* leaves could be a therapeutic agent in the treatment of liver disorders and oxidative stress.

As observed from this study, aggregation of these vital metabolites in different parts of *T. ciliata* suggest that the plant could be a potential therapeutic agent in the management of cancer, cardiovascular complications, cognitive impairment and other neurodegenerative disorders. Based on these findings, *T. ciliata* offers new perspectives for biofortification and food formulation using plant-based natural products. Hence, future studies may venture in the isolation, characterization and structural elucidation of these compounds in their pure forms to explore their utilization as drug precursors as well as their integration into functional foods.

5. Conclusions

Chemical profiling of metabolites aggregated in the crude extract of flower buds, leaves and root of *T. ciliata* was evaluated for the first time with UHPLC-MS, and 71 compounds were detected. Also, a maiden documentation of anticancer properties, acetylcholinesterase inhibition, and ROS scavenging activity of crude extracts of *T. ciliata* was achieved. Flower bud extracts prepared from 0 mM and 100 mM salinity treatments showed strong cytotoxicity to cancer cells, while they had moderate and weak cytotoxicity to non-cancer cells, respectively. All tested extracts possessed AChE inhibitory activities. Mainly, leaf extracts and root extracts from 0 mM salinity treatment demonstrated high ROS scavenging activity in liver cells. These findings suggest that *T. ciliata* could be exploited as a potential therapeutic agent for managing cancer, Alzheimer's disease, and liver disorders amidst the quest to develop more plant-based pharmaceuticals to treat chronic diseases. Therefore, results from this maiden study serve as a point of reference for future research avenues on the application of this species in the formulation of plant-based pharmaceuticals and functional foods. Further studies are recommended on the isolation and characterization of pure compounds from the species using nuclear magnetic resonance (NMR) to elucidate the chemical nature of isolated compounds and underpin the medicinal utilization of *T. ciliata*. The use of other solvents other than ethanol is recommended in future studies to expand the pharmacological potential of the species. Furthermore, clinical, in vivo, and *in silico* studies are also recommended in future research to validate findings from this study.

Data availability

The authors confirm that the datasets that support the findings are available on request through the corresponding author.

Funding

This work is based on the research supported in part by the National Research Foundation of South Africa ((Grant No. MND210624615237).

Ethical declaration

This work does not include any animal or human participants.

CRediT authorship contribution statement

Sihle Ngxabi: Writing – original draft, Methodology, Investigation, Formal analysis, Conceptualization. **Avela Sogoni:** Writing – review & editing, Visualization, Investigation. **Nasifu Kerebba:** Validation, Software, Resources, Methodology. **Rialet Pieters:** Writing – review & editing, Visualization, Validation, Resources, Methodology, Formal analysis. **Suranie Horn:** Writing – review & editing, Validation, Software, Resources, Methodology, Formal analysis. **John P. Giesy:** Writing – review & editing, Validation, Resources, Investigation. **Learnmore Kambizi:** Supervision, Resources, Project administration, Funding acquisition, Data curation. **Charles Petrus Laubscher:** Supervision, Resources, Project administration, Funding acquisition, Formal analysis. **Muhali Olaide Jimoh:** Writing – review & editing, Supervision, Software, Project administration, Formal analysis, Conceptualization.

Declaration of competing interest

The authors declare that they have no known competing financial interests or personal relationships that could have appeared to influence the work reported in this paper.

References

Aarts, J., Denison, M.S., De Haan, L.H.J., Schalk, J.A.C., Cox, M.A., Brouwer, A., 1993. Ah receptor-mediated luciferase expression: a tool for monitoring dioxin-like toxicity. Organohalogen Compd. 13, 361–364.

Abuzaid, H., Amin, E., Moawad, A., Ramadan Abdelmohsen, U., Hetta, M., Mohammed, R., 2020. Liquid chromatography high-resolution mass spectrometry analysis, phytochemical and biological study of two Aizoaceae plants: a new kaempferol derivative from Trianthema portulacastrum L. https://doi.org/10.4103/pr.pr_119_19.

Adetuyi, A.R., Ayenero, M.E., Olaleye, M.T., Akindahunsi, A.A., Akinmoladun, A.C., 2024a. Antioxidant and acetylcholinesterase inhibitory activities, in silico analyses, and anti-Alzheimer's disease potential of leaf extracts of three Nigerian endemic medicinal plants (Spondias mombin, Carica papaya and Kalanchoe crenata). Futur. J. Pharm. Sci. 10. https://doi.org/10.1186/s43094-023-00578-x.

Akay, M.B., Şener, K., Sari, S., Bodur, E., 2023. Inhibitory action of omega-3 and omega-6 fatty acids alpha-linolenic, arachidonic and linoleic acid on Human erythrocyte acetylcholinesterase. Protein J. 42, 96–103. https://doi.org/10.1007/s10930-022-10088-z.

ALNasser, M.N., Alboraiy, G.M., Alsowig, E.M., Alqattan, F.M., 2025. Cholinesterase inhibitors from plants and their potential in Alzheimer's treatment: systematic review. Brain Sci.. https://doi.org/10.3390/brainsci15020215.

Antunes-Ricardo, M., Guardado-Félix, D., Rocha-Pizaña, M.R., Garza-Martínez, J., Acevedo-Pacheco, L., Gutiérrez-Uribe, J.A., Villela-Castrejón, J., López-Pacheco, F., Serna-Saldívar, S.O., 2021. Opuntia ficus-indica extract and isorhamnetin-3-O-glucosyl-rhamnoside diminish tumor growth of colon cancer cells xenografted in immune-suppressed mice through the activation of apoptosis intrinsic pathway. Plant Foods Hum. Nutr. 76, 434–441. https://doi.org/10.1007/s11130-021-00934-3.

Asghar, S., Iqtadar, R., Azam, M., Author, C., 2025. Recent advances in acetylcholinesterase inhibitors for Alzheimer'S disease: a review of therapeutic strategies (1990-2024). Rev. J. Neurol. Med. Sci. Rev. 3. https://doi.org/10.63075/3txhyn76.

Asgharian, P., Tazekand, A.P., Hosseini, K., Forouhandeh, H., Ghasemnejad, T., Ranjbar, M., Hasan, M., Kumar, M., Beirami, S.M., Tarhriz, V., Soofiyani, S.R., Kozhamzharova, L., Sharifi-Rad, J., Calina, D., Cho, W.C., 2022. Potential mechanisms of quercetin in cancer prevention: focus on cellular and molecular targets. Cancer Cell Int. 22. https://doi.org/10.1186/s12935-022-02677-w.

Asong, J.A., Ndhlovu, P.T., Khosana, N.S., Aremu, A.O., Otang-Mbeng, W., 2019. Medicinal plants used for skin-related diseases among the Batswanas in Ngaka Modiri Molema District Municipality. S. Afr. S. Afr. J. Bot. 126, 11–20. https://doi.org/10.1016/j.sajb.2019.05.002.

Babashahi, S., Hansen, P., Sullivan, T., 2021. Creating a priority list of non-communicable diseases to support health research funding decision-making. Health Policy (N. Y.) 125, 221–228. https://doi.org/10.1016/J.HEALTHPOL.2020.12.003.

Bellanti, F., Coda, A.R.D., Trecca, M.I., Lo Buglio, A., Serviddio, G., Vendemiale, G., 2025. Redox imbalance in inflammation: the interplay of oxidative and reductive stress. Antioxidants 14. https://doi.org/10.3390/antiox14060656.

Boretti, A., 2023. Quercetin as a cancer chemopreventive or chemotherapeutic agent: where we stand. Phytother. Res. 37, 1227–1231. https://doi.org/10.1002/ptr.7699.

Bradford, M.M., 1976. A rapid and sensitive method for the quantitation of microgram quantities of protein utilizing the principle of protein-dye binding. Anal. Biochem. 72, 248–254. https://doi.org/10.1016/0003-2697(76)90527-3.

Calvano, C.D., Cataldi, T.R.I., Kögel, J.F., Monopoli, A., Palmisano, F., Sundermeyer, J., 2017. Structural characterization of neutral saccharides by negative ion MALDI mass spectrometry using a superbasic proton sponge as deprotonating matrix. J. Am. Soc. Mass Spectrom. 28, 1666–1675. https://doi.org/10.1007/s13361-017-1679-y.

Çetinkaya, M., Baran, Y., 2023. Therapeutic potential of luteolin on cancer. Vaccines 11. https://doi.org/10.3390/vaccines11030554.

Chen, J., Li, C., Bu, C.L.N., Wang, Y., Qi, M., Fu, P., Zeng, X., 2025. Global burden of non-communicable diseases attributable to kidney dysfunction with projection into 2040. Chin. Med. J. 138, 1334–1344. https://doi.org/10.1097/CM9.0000000000003143.

Chen, Z.R., Huang, J.B., Yang, S.L., Hong, F.F., 2022. Role of cholinergic signaling in Alzheimer's disease. Molecules. https://doi.org/10.3390/molecules27061816.

Cichon, N., Grabowska, W., Gorniak, L., Stela, M., Harmata, P., Ceremuga, M., Bijak, M., 2025a. Mechanistic and therapeutic insights into flavonoid-based inhibition of acetylcholinesterase: implications for neurodegenerative diseases. Nutrients 17. https://doi.org/10.3390/nu17010078.

Cichon, N., Grabowska, W., Gorniak, L., Stela, M., Harmata, P., Ceremuga, M., Bijak, M., 2025b. Mechanistic and therapeutic insights into flavonoid-based inhibition of acetylcholinesterase: implications for neurodegenerative diseases. Nutrients 17. https://doi.org/10.3390/nu17010078.

Cock, I., Mavuso, N., Van Vuuren, S., 2021. A review of plant-based therapies for the treatment of urinary tract infections in traditional Southern African medicine. Evid.-based Complement. Altern. Med. https://doi.org/10.1155/2021/7341124, 2021.

Cock, I.E., 2015. The genus aloe: phytochemistry and therapeutic uses including treatments for gastrointestinal conditions and chronic inflammation, in: Rainsford, K.D., Powanda, M.C., Whitehouse, M.W. (Eds), Progress in Drug Research. Springer, Sheffield, pp. 179–235.

de Oliveira, P.C.O., da Silva, G.M., Cass, Q.B., de Moraes, M.C., Cardoso, C.L., 2024. Natural products as a source of cholinesterase inhibitors. Pharmacol. Res. - Nat. Prod. 5, 100099. https://doi.org/10.1016/J.PRENAP.2024.100099.

De Vynck, J.C., Van Wyk, B.E., Cowling, R.M., 2016. Indigenous edible plant use by contemporary Khoe-San descendants of South Africa's Cape South Coast. S. Afr. J. Bot. 102, 60–69. https://doi.org/10.1016/j.sajb.2015.09.002.

Dicks, L.M.T., 2024. Cardiovascular disease may Be triggered by gut microbiota, microbial metabolites, gut wall reactions, and inflammation. Int. J. Mol. Sci. 25. https://doi.org/10.3390/ijms251910634.

Eid, R.A., Abadi, A.M., Alghamdi, M.A., El-kott, A.F., Mohamed, G., Al-Shraim, M., Alaa Eldeen, M., Zaki, M.S.A., Shalaby, F.M., 2024. Echinops Asteraceae extract guards against malathion-induced liver damage via minimizing oxidative stress, inflammation, and apoptosis. Toxicon. 244, 107750. https://doi.org/10.1016/J.TOXICON.2024.107750.

Ejiofor, E.U., Oyedemi, S.O., Onoja, S.O., Omeh, N.Y., 2022. Amaranthus hybridus Linn. Leaf extract ameliorates oxidative stress and hepatic damage abnormalities induced by thioacetamide in rats. S. Afr. J. Bot. 146, 213–221. https://doi.org/10.1016/J.SAJB.2021.10.029.

Ellman, G.L., Courtney, K.D., Andres, V., Featherstone, R.M., 1961. A new and rapid colorimetric determination of acetylcholinesterase activity. Biochem. Pharmacol. 7, 88–95. https://doi.org/10.1016/0006-2952(61)90145-9.

Engelbrecht, I., Suranie, H., Giesy, J.P., Pieters, R., 2024. A method to determine reactive oxygen species production in intestinal and liver cell cultures using the 2',7'-dichlorodihydrofluorescein diacetate assay. MethodsX. 12, 102615. https://doi.org/10.1016/S0891-5849(99)00, 107-0.

Ferreira, M.J., Pinto, D.C.G.A., Cunha, Â., Silva, H., 2022. Halophytes as medicinal plants against Human infectious diseases. Appl. Sci. (Switz.) 12, 7493. https://doi.org/10.3390/app12157493.

Ferreres, F., Andrade, P.B., Valentão, P., Gil-Izquierdo, A., 2008. Further knowledge on barley (Hordeum vulgare L.) leaves O-glycosyl-C-glycosyl flavones by liquid chromatography-UV diode-array detection-electrospray ionisation mass spectrometry. J. Chromatogr. A 1182, 56–64. https://doi.org/10.1016/J.CHROMA.2007.12.070.

Gajendra, K., Pratap, G.K., Poornima, D.V., Shantaram, M., Ranjita, G., 2024. Natural acetylcholinesterase inhibitors: a multi-targeted therapeutic potential in Alzheimer's disease. Eur. J. Med. Chem. Rep. 11, 100154. https://doi.org/10.1016/J.EJMCR.2024.100154.

Gao, X.Y., Li, X.Y., Zhang, C.Y., Bai, C.Y., 2024. Scopoletin: a review of its pharmacology, pharmacokinetics, and toxicity. Front. Pharmacol. 15. https://doi.org/10.3389/fphar.2024.1268464.

Gonfa, Y.H., Tessema, F.B., Bachheti, A., Rai, N., Tadesse, M.G., Nasser Singab, A., Chaubey, K.K., Bachheti, R.K., 2023. Anti-inflammatory activity of phytochemicals from medicinal plants and their nanoparticles: a review. Curr. Res. Biotechnol. 6, 100152. https://doi.org/10.1016/J.CRBIOT.2023.100152.

Gong, G., Guan, Y.Y., Zhang, Z.L., Rahman, K., Wang, S.J., Zhou, S., Luan, X., Zhang, H., 2020. Isorhamnetin: A review of Pharmacological Effects. Biomedicine and Pharmacotherapy. https://doi.org/10.1016/j.biopha.2020.110301.

González-Barrio, R., Periago, M.J., Luna-Recio, C., Garcia-Alonso, F.J., Navarro-González, I., 2018. Chemical composition of the edible flowers, pansy (Viola wittrockiana) and snapdragon (Antirrhinum majus) as new sources of bioactive compounds. Food Chem. 252, 373–380. https://doi.org/10.1016/J.FOODCHEM.2018.01.102.

Grabarics, M., Lettow, M., Kirschbaum, C., Greis, K., Manz, C., Pagel, K., 2022. Mass spectrometry-based techniques to elucidate the sugar code. Chem. Rev. 122, 7840–7908. https://doi.org/10.1021/acs.chemrev.1c00380.

Hanumanthappa, R., Kadandelu, M., Raghu, S.V., Devaraju, K.S., 2024. Estimation of total proteins in Drosophila using the Bradford method, in: Lakhotia, S.C., Ranganath, H.A. (Eds), Experiments With Drosophila for Biology Courses. Indian Academy of Sciences Bengaluru, Bengaluru, India.

Härtl, R., Gleinich, A., Zimmermann, M., 2011. Dramatic increase in readthrough acetylcholinesterase in a cellular model of oxidative stress. J. Neurochem. 116, 1088–1096. https://doi.org/10.1111/j.1471-4159.2010.07164.x.

Huang, Q., Liao, C., Ge, F., Ao, J., Liu, T., 2022. Acetylcholine bidirectionally regulates learning and memory. J. Neurorestoratol. 10, 100002. https://doi.org/10.1016/J.JNRT.2022.100002.

Huete-Acevedo, J., Mas-Bargues, C., Arnal-Forné, M., Atencia-Rabadán, S., Sanz-Ros, J., Borrás, C., 2024. Role of redox homeostasis in the communication between brain and liver through extracellular vesicles. Antioxidants 13. https://doi.org/10.3390/antiox13121493.

Idris, O.A., Kerebba, N., Horn, S., Maboeta, M.S., Pieters, R., 2023. Phytochemical-based evidence of the health benefits of Bidens Pilosa extracts and cytotoxicity. Chem. Afr. 6, 1767–1788. https://doi.org/10.1007/s42250-023-00626-2.

International Organisation for Standardisation (ISO), 2009. Biological Evaluation of Medical Devices —Part 5: Tests for in Vitro Cytotoxicity. ISO, Geneva.

Islam, M.T., Aktaruzzaman, M., Saif, A., Hasan, A.R., Sourov, M.M.H., Sikdar, B., Rehman, S., Tabassum, A., Abeed-Ul-Haque, S., Sakib, M.H., Muhib, M.M.A., Setu, M.A.A., Tasnim, F., Rayhan, R., Abdel-Daim, M.M., Raihan, M.O., 2024. Identification of acetylcholinesterase inhibitors from traditional medicinal plants for Alzheimer's disease using in silico and machine learning approaches. RSC. Adv. 14, 34620–34636. https://doi.org/10.1039/d4ra05073h.

Jeong, J.H., An, J.Y., Kwon, Y.T., Rhee, J.G., Lee, Y.J., 2009. Effects of low dose quercetin: cancer cell-specific inhibition of cell cycle progression. J. Cell Biochem. 106, 73–82. https://doi.org/10.1002/jcb.21977.

Jiang, J., Zhu, F., Zhang, H., Sun, T., Fu, F., Chen, X., Zhang, Y., 2022. Luteolin suppresses the growth of colon cancer cells by inhibiting the IL-6/STAT3 signaling pathway. J. Gastrointest. Oncol. 13, 1722–1732. https://doi.org/10.21037/JGO-22-507/COIF.

Jimoh, M.A., Jimoh, M.O., Bello, M., Raimi, I.O., Okunlola, G.O., Mkhwanazi, N., Laubscher, C.P., 2024. In vitro anti-HIV, cytotoxicity and nutritional analysis of Trianthema portulacastrum L. (Aizoaceae). BMC. Complement. Med. Ther. 24. https://doi.org/10.1186/s12906-023-04300-5.

Jimoh, M.O., Kerebba, N., Okechukwu, O.C., Jimoh, A.A., Salaudeen, T., Bamigboye, S. O., Sogoni, A., Okaiyeto, K., Mkhwanazi, N., Kadye, R., Idris, O.A., Erasmus, M., Prinsloo, E., Laubscher, C.P., 2024. Analysis of antioxidant nutrients, anti-HIV and anticancer metabolic fingerprints of pelargonium quercifolium (L.f) L'Hér. Food Chem. Adv. 5. https://doi.org/10.1016/j.focha.2024.100804.

Karunakaran, K.B., Thiyagaraj, A., Santhakumar, K., 2022. Novel insights on acetylcholinesterase inhibition by Convolvulus pluricaulis, scopolamine and their combination in zebrafish. Nat. Prod. Bioprospect. 12. https://doi.org/10.1007/s13659-022-00332-5.

Kaushik, V., Smith, S.T., Mikobi, E., Raji, M.A., 2018. Acetylcholinesterase inhibitors: beneficial effects on comorbidities in patients with Alzheimer's disease. Am. J. Alzheimers. Dis. Other Demen. 33, 73–85. https://doi.org/10.1177/1533317517734352.

Kim, D.K., Lee, K., 2003. ~[rtljibe~ of barmacaI ~e~eartb inhibitory effect of trans-N-p-coumaroyl tryamine from the twigs of Celtis chinensis on the acetylcholinesterase. Arch. Pharm. Res. 26, 735–738. https://doi.org/10.1007/bf02976684.

Kim, J.H., Kismali, G., Gupta, S.C., 2018. Natural Products for the prevention and treatment of chronic inflammatory diseases: integrating traditional medicine into modern chronic diseases care. Evid.-based Complement. Altern. Med. https://doi.org/10.1155/2018/9837863, 2018.

Kouhestani, S., Jafari, A., Babaei, P., 2018. Kaempferol attenuates cognitive deficit via regulating oxidative stress and neuroinflammation in an ovariectomized rat model of sporadic dementia. Neural Regen. Res. 13, 1827–1832. https://doi.org/10.4103/1673-5374.238714.

Lebel, C.P., Ischiropoulos, H., Bondy8, S.C., 1992. Evaluation of the probe 2',7'-dichlorofluorescin as an indicator of reactive oxygen species formation and oxidative stress. Chem. Res. Toxicol 5, 227–231. https://doi.org/10.1021/tx00026a012.

Lee, J., Kim, J., Lee, R., Lee, E., Choi, T.G., Lee, A.S., Yoon, Y.I., Park, G.C., Namgoong, J. M., Lee, S.G., Tak, E., 2022. Therapeutic strategies for liver diseases based on redox control systems. Biomed. Pharmacother. 156, 113764. https://doi.org/10.1016/J.BIOPHA.2022.113764.

Lee, J.H., Park, M.J., Ryu, H.W., Yuk, H.J., Choi, S.W., Lee, K.S., Kim, S.L., Seo, W.D., 2016. Elucidation of phenolic antioxidants in barley seedlings (Hordeum vulgare L.) by UPLC-PDA-ESI/MS and screening for their contents at different harvest times. J. Funct. Foods. 26, 667–680. https://doi.org/10.1016/J.JFF.2016.08.034.

Lee, K.Y., Nam, D.H., Jeon, Y., Park, S.U., Cho, J., Gulandaz, M.A., Chung, S.O., Lee, G.J., 2024. Exploring the production of secondary metabolites from a halophyte Tetragonia tetragonoides through Callus Culture. Horticulturae 10. https://doi.org/10.3390/horticulturae10030244.

Liao, Y., Mai, X., Wu, X., Hu, X., Luo, X., Zhang, G., 2022. Exploring the inhibition of quercetin on acetylcholinesterase by multispectroscopic and In silico approaches and evaluation of its neuroprotective effects on PC12 cells. Molecules. 27. https://doi.org/10.3390/molecules27227971.

Lin, H., Wang, X., Zhao, J., Lin, Z., 2023. Protective effect of kaempferol against cognitive and neurological disturbances induced by D-galactose and aluminum chloride in mice. J. Funct. Foods. 100, 105385. https://doi.org/10.1016/J.JFF.2022.105385.

Liu, J., Li, T., Zhong, G., Pan, Y., Gao, M., Su, S., Liang, Y., Ma, C., Liu, Y., Wang, Q., Shi, Q., 2023. Exploring the therapeutic potential of natural compounds for Alzheimer's disease: mechanisms of action and pharmacological properties. Biomed. Pharmacother. 166, 115406. https://doi.org/10.1016/J.BIOPHA.2023.115406.

López-García, J., Lehocký, M., Humpolíček, P., Sáha, P., 2014. HaCaT keratinocytes response on antimicrobial atelocollagen substrates: extent of cytotoxicity, cell viability and proliferation. J. Funct. Biomater. 5, 43–57. https://doi.org/10.3390/jfb5020043.

Lucero-Prisno, D.E., Shomuyiwa, D.O., Kouwenhoven, M.B.N., Dorji, T., Odey, G.O., Miranda, A.V., Ogunkola, I.O., Adebisi, Y.A., Huang, J., Xu, L., Obnial, J.C., Huda, A., Thepanondh, S., Dayrit, M.M., Evardone, S.B., Lamawansa, M.D., Solomon Ethiopia, S., Aziato, L., Adongo, P.B., Samai, M.H., Garcia, F.B., Villaruz, J.F., Karunathilake, I.M., Li, H., Azanza, P.A., Findlay, I., Wong, M.C.S., 2023. Top 10 public health challenges to track in 2023: shifting focus beyond a global pandemic. Public Health Chall. 2. https://doi.org/10.1002/puh2.86.

Marucci, G., Buccioni, M., Ben, D.D., Lambertucci, C., Volpini, R., Amenta, F., 2021. Efficacy of acetylcholinesterase inhibitors in Alzheimer's disease. Neuropharmacology. 190, 108352. https://doi.org/10.1016/J.NEUROPHARM.2020.108352.

Mattia, C.J., Lebel, C.P., Bondy, S.C., 1991. Effects of toluene and its metabolites on cerebral reactive oxygen species generation. Biochem. Pharmacol. 42, 879–882. https://doi.org/10.1016/0006-2952(91)90048-A.

Meilawati, L., Dewi, R., Tasfiyati, A., Septama, A., Antika, L.D., 2023. Scopoletin: anticancer potential and mechanism of action. Asian Pac. J. Trop. Biomed. 13, 1–8. https://doi.org/10.4103/2221-1691.367685.

Mohammed, H.A., Emwas, A.H., Khan, R.A., 2023. Salt-tolerant plants, halophytes, as renewable natural resources for cancer prevention and treatment: roles of phenolics and flavonoids in immunomodulation and suppression of oxidative stress towards cancer management. Int. J. Mol. Sci. 24. https://doi.org/10.3390/ijms24065171.

Ngxabi, S., Jimoh, M.O., Laubscher, C.P., Kambizi, L., 2024. Leaf micromorphological assessment, chemical composition and anatomical responses of Trachyandra ciliata (L.F) Kunth to different degrees of salinity. Russ. J. Plant Physiol. 71, 112. https://doi.org/10.1134/S1021443723603695.

Ngxabi, S., Jimoh, M.O., Sogoni, A., Laubscher, C.P., Rautenbach, F., Kambizi, L., 2025. Salinity influenced proximate, minerals, anti-nutrients and phytochemical composition of Trachyandra ciliata Kunth (Wild Cabbage): a promising edible halophyte. Food Sci. Nutr. 13. https://doi.org/10.1002/fsn3.4755.

Orhan, I.E., 2020. Cholinesterase inhibitory potential of quercetin towards Alzheimer's disease - A promising natural molecule or fashion of the day? - A narrowed review. Curr. Neuropharmacol. 19, 2205–2213. https://doi.org/10.2174/1570159×18666201119153807.

Patel, A.B., 2023. Simple and rapid colorimetric method for determination of erythrocyte and plasma cholinesterase activities and comparison with the standard Ellman's method. Public Health Toxicol. 3, 1–10. https://doi.org/10.18332/pht/172229.

Piovani, D., Nikolopoulos, G.K., Bonovas, S., 2022. Non-communicable diseases: the invisible epidemic. J. Clin. Med. 11. https://doi.org/10.3390/jcm11195939.

Pupyshev, A.B., Akopyan, A.A., Tenditnik, M.V., Ovsyukova, M.V., Dubrovina, N.I., Belichenko, V.M., Korolenko, T.A., Zozulya, S.A., Klyushnik, T.P., Tikhonova, M.A., 2024. Alimentary treatment with trehalose in a pharmacological model of Alzheimer's disease in mice: effects of different dosages and treatment regimens. Pharmaceutics. 16. https://doi.org/10.3390/pharmaceutics16060813.

Rivera-Pastrana, D.M., Yahia, E.M., González-Aguilar, G.A., 2010. Phenolic and carotenoid profiles of papaya fruit (Carica papaya L.) and their contents under low temperature storage. J. Sci. Food Agric. 90, 2358–2365. https://doi.org/10.1002/jsfa.4092.

Safiri, S., Ghaffari Jolfayi, A., Fazlollahi, A., Morsali, S., Sarkesh, A., Daei Sorkhabi, A., Golabi, B., Aletaha, R., Motlagh Asghari, K., Hamidi, S., Mousavi, S.E., Jamalkhani, S., Karamzad, N., Shamekh, A., Mohammadinasab, R., Sullman, M.J.M., Şahin, F., Kolahi, A.A., 2024. Alzheimer's disease: a comprehensive review of epidemiology, risk factors, symptoms diagnosis, management, caregiving, advanced treatments and associated challenges. Front. Med. (Lausanne) 11. https://doi.org/10.3389/fmed.2024.1474043.

Schulze, R.J., Schott, M.B., Casey, C.A., Tuma, P.L., McNiven, M.A., 2019. The cell biology of the hepatocyte: a membrane trafficking machine. J. Cell Biol. 218, 2096–2112. https://doi.org/10.1083/jcb.201903090.

Serag, A., Baky, M.H., Döll, S., Farag, M.A., 2019a. UHPLC-MS metabolome based classification of umbelliferous fruit taxa: a prospect for phyto-equivalency of its different accessions and in response to roasting. RSC. Adv. 10, 76–85. https://doi.org/10.1039/c9ra07841j.

Serag, A., Ion-Margineanu, A., Qureshi, H., McMillan, R., Saint Martin, M.J., Diamond, J., O'Reilly, P., Hamilton, P., 2019b. Translational AI and deep learning in Diagnostic pathology. Front. Med. (Lausanne) 26, 246. https://doi.org/10.3389/fmed.2019.00185.

Shen, W.K., Sheldon, R.S., Benditt, D.G., Cohen, M.I., Forman, D.E., Goldberger, Z.D., Grubb, B.P., Hamdan, M.H., Krahn, A.D., Link, M.S., Olshansky, B., Raj, S.R., Sandhu, R.K., Sorajja, D., Sun, B.C., Yancy, C.W., 2017. 2017 ACC/AHA/HRS Guideline for the evaluation and management of patients with syncope: a report of the American College of Cardiology/American Heart Association Task Force on Clinical Practice Guidelines and the Heart Rhythm Society. J. Am. Coll. Cardiol. 70, e39–e110. https://doi.org/10.1016/j.jacc.2017.03.003.

Siegel, R.L., Miller, K.D., Jemal, A., 2019. Cancer statistics, 2019. CA Cancer J. Clin. 69, 7–34. https://doi.org/10.3322/caac.21551.

Sies, H., 2015. Oxidative stress: a concept in redox biology and medicine. Redox. Biol. 4, 180–183. https://doi.org/10.1016/J.REDOX.2015.01.002.

Sogoni, A., Jimoh, M.O., Kerebba, N., Ngxabi, S., Giesy, J.P., Pieters, R., Horn, S., Kambizi, L., Laubscher, C.P., 2025a. Phytochemical profiling of saline cultivated Tetragonia decumbens Mill: in vitro cytotoxicity, acetylcholinesterase inhibitory activity, anti-cancer and anti-inflammatory potential. S. Afr. J. Bot. 186, 422–435. https://doi.org/10.1016/J.SAJB.2025.09.010.

Sogoni, A., Jimoh, M.O., Ngxabi, S., Kambizi, L., Laubscher, C.P., 2025b. Evaluating the nutritional, therapeutic, and economic potential of Tetragonia decumbens Mill.: a promising wild leafy vegetable for bio-saline agriculture in South Africa. Open. Agric. 10. https://doi.org/10.1515/opag-2022-0368.

Song, J., Zhang, H., Wang, Z., Wang, J., 2022. The antioxidant activity, α-glucosidase and acetylcholinesterase inhibition activity, and chemical composition of Paeonia delavayi petal. Food Qual. Saf. 6. https://doi.org/10.1093/fqsafe/fyac020.

Tan, W.S., Arulselvan, P., Ng, S.F., Taib, C.N.M., Sarian, M.N., Fakurazi, S., 2020. Healing effect of Vicenin-2 (VCN-2) on Human dermal fibroblast (HDF) and development VCN-2 hydrocolloid film based on Alginate as potential wound dressing. Biomed. Res. Int. https://doi.org/10.1155/2020/4730858, 2020.

Taqui, R., Debnath, M., Ahmed, S., Ghosh, A., 2022. Advances on plant extracts and phytocompounds with acetylcholinesterase inhibition activity for possible treatment of Alzheimer's disease. Phytomed. Plus 2, 100184. https://doi.org/10.1016/J.PHYPLU.2021.100184.

Touhtouh, J., Laghmari, M., Chraa, F., Benali, T., Ghanam, J., El Shazly, M., Goh, K.W., Bouyahya, A., Lee, L.H., Aanniz, T., Hammani, K., 2025. Celtis genus (Cannabaceae): a comprehensive review of the ethnomedicinal use, food value, phytochemistry, biological activities, valuable compounds, and insight into mechanisms of action. J. Agric. Food Res. https://doi.org/10.1016/j.jafr.2025.101797.

Venkatachalapathy, D., Shivamallu, C., Prasad, S.K., Thangaraj Saradha, G., Rudrapathy, P., Amachawadi, R.G., Patil, S.S., Syed, A., Elgorban, A.M., Bahkali, A. H., Kollur, S.P., Basalingappa, K.M., Bajek, A., Roszkowski, K., 2021. molecules assessment of chemopreventive potential of the plant extracts against liver cancer using HepG2 cell line. Molecules. https://doi.org/10.3390/molecules26154593.

Viana, M.D.M., Lauria, P.S.S., Lima, A.A.de, Opretzka, L.C.F., Marcelino, H.R., Villarreal, C.F., 2022. Alpha-Lipoic Acid as an Antioxidant Strategy For Managing Neuropathic Pain. Antioxidants. https://doi.org/10.3390/antiox11122420.

Wang, H., Chen, Lijia, Yang, B., Du, J., Chen, Liang, Li, Y., Guo, F., 2023. Structures, sources, identification/quantification methods, health benefits, bioaccessibility, and products of isorhamnetin glycosides as phytonutrients. Nutrients. 15. https://doi.org/10.3390/nu15081947.

Yang, Z., Zou, Y., Wang, L., 2023. Neurotransmitters in prevention and treatment of Alzheimer's disease. Int. J. Mol. Sci. https://doi.org/10.3390/ijms24043841.

Ye, M., Yan, Y., Guo, D.A., 2005. Characterization of phenolic compounds in the Chinese herbal drug Tu-Si-Zi by liquid chromatography coupled to electrospray ionization

mass spectrometry. Rapid Commun. Mass Spectrom. 19, 1469–1484. https://doi.org/10.1002/rcm.1944.

Yoshizane, C., Mizote, A., Arai, C., Arai, N., Ogawa, R., Endo, S., Mitsuzumi, H., Ushio, S., 2020. Daily consumption of one teaspoon of trehalose can help maintain glucose homeostasis: a double-blind, randomized controlled trial conducted in healthy volunteers. Nutr. J. 19. https://doi.org/10.1186/s12937-020-00586-0.

Zafar, A., Khatoon, S., Khan, M.J., Abu, J., Naeem, A., 2025. Advancements and limitations in traditional anti-cancer therapies: a comprehensive review of surgery, chemotherapy, radiation therapy, and hormonal therapy. Discov. Oncol. 16. https://doi.org/10.1007/s12672-025-02198-8.

Zavala-Ocampo, L.M., Aguirre-Hernández, E., López-Camacho, P.Y., Cárdenas-Vázquez, R., Dorazco-González, A., Basurto-Islas, G., 2022. Acetylcholinesterase inhibition and antioxidant activity properties of Petiveria alliacea L. J. Ethnopharmacol. 292, 115239. https://doi.org/10.1016/J.JEP.2022.115239.

Zhang, H., Wang, K., Wu, J., Chen, Y., He, P., 2011. A new flavonoid glycoside from Vaccaria hispanica. Nat. Prod. Commun. 6, 1599–1602. https://doi.org/10.1177/1934578×1100601112.

Zhang, J., Ma, Y., 2024. Luteolin as a potential therapeutic candidate for lung cancer: emerging preclinical evidence. Biomed. Pharmacother. 176, 116909. https://doi.org/10.1016/j.biopha.2024.116909.

Zhang, V.X., Sze, K.M.F., Chan, L.K., Ho, D.W.H., Tsui, Y.M., Chiu, Y.T., Lee, E., Husain, A., Huang, H., Tian, L., Wong, C.C.L., Ng, I.O.L., 2021. Antioxidant supplements promote tumor formation and growth and confer drug resistance in hepatocellular carcinoma by reducing intracellular ROS and induction of TMBIM1. Cell Biosci. 11. https://doi.org/10.1186/s13578-021-00731-0.

Zhao, X., Zhang, S., Liu, D., Yang, M., Wei, J., 2020. Analysis of flavonoids in dalbergia odorifera by ultra-performance liquid chromatography with tandem mass spectrometry. Molecules 25. https://doi.org/10.3390/molecules25020389.